CHAPTER 4
RESULTS ANALYSIS

4.1 INTRODUCTION

It was noted from the few published researches in literature that there is a lack of knowledge in understanding the chemical, the physical, pozzolanic reactivity and mineral characterization of dealuminated kaolin (DK) as a waste by-product material.

Most of studies carried out with DK as a pozzolanic material were focused in DK/lime systems (Mostafa et al, 2001a and Mostafa et al, 2001b). However, there is a lack of investigations about the reaction kinetics in DK-blended cement. It is well known that the chemical reactions taking place in blended cement containing any type of pozzolan are generally more complex than in pozzolan/lime system (Frías and Cabrera, 2001). This attributed to the fact that cement is a mixture of phases reacting at different rates. This fact in conjunction with the presence of other compounds, such as sulphate, alkali, chlorides and minor element (zinc, cadmium, lead, chromium, etc.), could provoke an alteration in the pozzolanic reaction rate and, therefore in the development of hydrated phases.

Microstructure-property relationships are at the heart of modern material science. Although concrete is the most widely used structural material, its microstructure is highly heterogeneous and complex. The effect of DK inclusion as a relatively new pozzolanic material on the microstructure OPC paste has not been investigated yet. Therefore, it is very important to have a good understanding about this effect, in order to understand fluid transport properties and hence developing durable concrete. Moreover, the morphology of the solid hydration products of OPC/DK paste have not been investigated yet. Therefore, it is very essential to investigate the microstructure of the ITZ between the aggregate and OPC/DK paste before using DK in concrete industry as a cement replacement material. These sorts of investigation helps in determining and interpreting the role of DK inclusion in OPC concrete.

The specific surface area and the pozzolanic activity of any cement replacement material when partially replaced by cement may lead to change in the amount of water demand during fresh state. Moreover its addition will affect on other fresh parameters, such as flowability,

rate of flowability loss and rheology occurring during the fresh state. However, the effect of inclusion of DK into OPC matrix on these properties has not been investigated yet.

To the author's knowledge, there is no work has been done in the literature regarding the effect of DK on the mechanical, fluid transport properties of OPC matrices. Consequently, there is a great need for an experimental work to study the effect of incorporating DK with different replacement levels on the hardened (compressive, direct tensile, splitting, flexural strengths, stress-strain behavior and shrinkage) and fluid transport properties of OPC matrix to specify the optimum DK content that would be utilized in the OPC concrete mixes.

It was concluded from the literature that dealuminated kaolin can be considered as a good candidate to be used as additive in blended cements (Mostafa et al, 2001a). However, it contains about 9.0% amorphous Al_2O_3 in the bulk chemical composition for DK. This may change the chemistry of DK–cement hydration reaction or the long-term stability of concrete. The later effect may be caused by the potential formation of ettringite in sulphate media due to the high Al_2O_3 content. Therefore, it is very essential to investigate the effect of DK incorporation on durability of OPC matrix subjected to sulphate environment. Moreover, it is very important to investigate the suitability of exploiting DK as a cement replacement material in reinforced concrete industry. This could be achieved by studying the effect of DK incorporation on corrosion of reinforced OPC matrix exposed to chloride environment. Therefore, this chapter was undertaken to gain an improved understanding of the above-mentioned aspects.

4.2 CHARACTERIZATION OF THE MATERIALS

4.2.1 The Dealuminated Kaolin

4.2.1.1 Chemical composition

The chemical analyses of as received DK (DKut) as well as of the treated sample (DKt) are shown in Table 3.1. The results indicate that the SiO_2 content of the DKut and DKt is equal to 72 and 64%, respectively. The percentage of alumina (Al_2O_3) amounts varies from 13 and 16%, and the Fe_2O_3 lay in the range of 2 and 1% in both samples respectively. The CaO concentration is higher in the DKt than that in DKut and shows values of 6.63 and 2.84%, respectively. The concentrations of MgO and alkali oxides are low in the samples and show values of 0.3 and ~ 0.02%, respectively. The sulfate content (SO^-_3) lays in the range of 3 to 3.4%. Both samples lose 6 to 7% upon ignition.

Table 4.1 Chemical analysis of DKut, DKt and SF.

Oxide content, % by mass	DKut	DKt	SF
SiO_2	72.10	64.8	96.4
Al_2O_3	13.00	16.0	0.77
Fe_2O_3	2.01	1.00	1.05
CaO	2.84	6.63	0.07
MgO	0.30	0.36	0.03
Na_2O	0.13	0.02	0.06
K_2O	0.02	0.02	0.24
SO^-_3	3.08	3.42	0.60
Loss on ignition (L.O.I)	6.1	7.16	1.21

4.2.1.2 X-ray diffraction

The X-ray diffractograms of the untreated and treated dealuminated kaolin sample are illustrated in Figure 4.1. The as received sample (DKut) is composed mainly of quartz (SiO_2) with a small proportion of titanium oxide (TiO_2) and gypsum ($CaSO_4.2H_2O$). A considerable amount of amorphous material is present in the sample as indicated from the hump observed around 2 theta equal to 20-25 degrees. The sample treated with lime (DKt) is composed of an appreciable amount of hemihydrate.

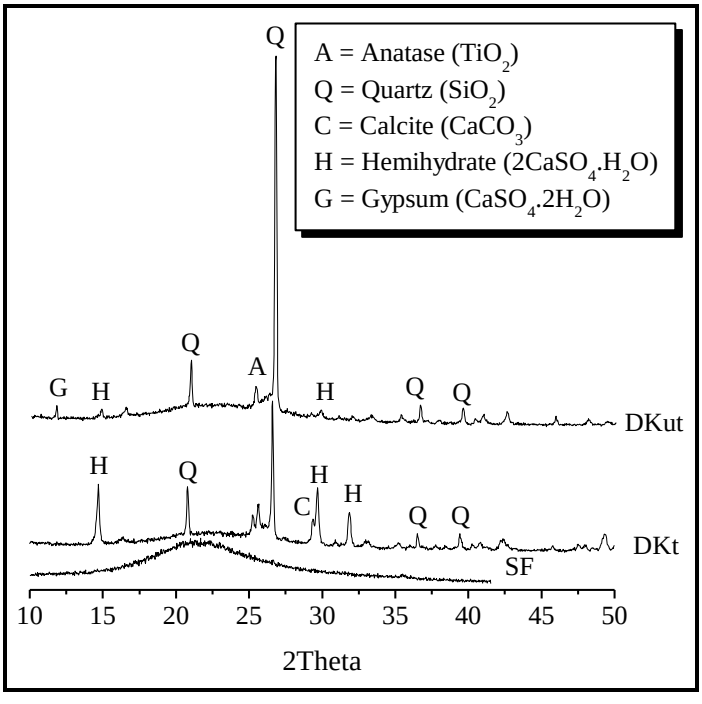

Figure 4.1 X-ray diffractograms of DKut, DKt and SF.

4.2.1.3 Pozzolanic reactivity

The results obtained from the pozzolanic reactivity of the untreated and treated DK are shown in Table 4.2; the values obtained are expressed relative to the reactivity of the silica fumes. The table shows that the reactivity of the as received samples is 127% higher than that of the silica fumes, that of the treated is slightly lower and amounts to 117% relative to the silica fumes.

Table 4.2 Pozzolanic activity and physical properties of DKut and DKt

Properties	**DKut**	**DKt**
Pozzolanic reactivity, (% relative to the silica fumes)	127	117
BET specific surface area, (m^2/gm)	42	40.1
Density, (gm/cm^3)	1.95	2.1

4.2.1.4 Surface area measurements and specific gravities

Table 4.2 illustrates further that BET surface areas of the DKut and DKt are found to be 42m^2/gm and 40.1 m^2/g and their densities 1.95 and 2.1 g/cc for DKut and DKt, respectively.

4.2.2 Silica fume

The chemical analysis of the silica fume is given in Table 4.1 and shows that it consist of 96% silica, the remaining 4% are composed of alumina, ferric oxide, magnesia, calcium, alkalies and sulfur oxides. The X-ray diffractogram shown in Figure 4.1 illustrates that the silica fume (SF) is completely amorphous material. The BET surface area of the silica fume amounts to 20 m^2/g. and its specific gravity to 2.3 g/cc.

4.2.3 Ordinary Portland Cement

4.2.3.1 Chemical composition and physical properties

Table 4.3 illustrates the chemical and physical properties of the ordinary Portland cement used. The results show that the cement composition and properties lay within the standard specification.

Table 4.3 Chemical composition and Physical properties of OPC

a- Chemical Composition, %	**a- Chemical Composition, %**	
	SiO_2	20.56
	Al_2O_3	5.59
	Fe_2O_3	2.65
	CaO	63.13
	MgO	1.94
	Na_2O	0.43
	K_2O	0.22
	SO_3	2.69
	Loss on ignition (L.O.I)	2.61
	Insoluble residue	0.87
b-Bogue Compound Composition, %	**b- Bogue Compound Composition, %**	
	C_3S	61.00
	C_2S	12.70
	C_3A	10.30
	C_4AF	9.10
c- Physical Properties	**c- Physical Properties**	
	Setting time, min. Initial	110
	Final	155
	Standard water requirement, cm^3	112
	Compressive strength, Kg/cm^2	
	3-days	250
	7-days	350
	Specific surface, Blaine, m^2/kg	370
	Specific surface, BET, m^2/g	-

4.2.4 Aggregates

Table 4.4 shows the grading and physical properties of the aggregates used and indicate their compliance with the standard specifications (ESS 1109,1971).

Table 4.4 Grading and physical properties of aggregate.

Sieve size, mm	% Passing	
	Gravel	**Sand**
25.0	100.00	100.00
19.0	100.00	100.00
13.2	60.00	100.00
9.5	45.00	100.00
4.75	-	100.00
2.36	-	94.50
1.18	-	83.30
0.6	-	73.2
0.425	-	30.50
0.3	-	8.00
0.15	-	2.00
0.075	-	1.00
Pan	-	0.00
Physical properties		
Max. Nominal Size, mm	19.00	-
Fineness Modulus	-	2.4
Volumetric Weight (Oven dry), t/m^3	1.70	1.60
Apparent specific gravity	2.65	2.60
Absorption Capacity, %	0.9	0.7

4.3 CEMENT PASTE

4.3.1 The Effect of DKut and DKt on the pH Value of the Cement Slurry

As previously mentioned in 3.1.8.1, the as received DKut was acidic; its slurry showed a pH-value =4.5; the pH-value of the slurry made of the DKt was raised to 7.0 through its neutralization with lime. Because the present investigation deals with the DK as an OPC replacement material, the effect of their addition on the pH value of cement was studied, as shown in Figure 4.2. It is clear from the figure that at zero time the pH-value of cement slurry decreases significantly with DKut addition but increases again upon standing and attains a complete leveling after 90 minutes. On the other hand, the depression in the pH-values of the cement slurries upon the addition of the DKt is lower than that in the case of DKut.

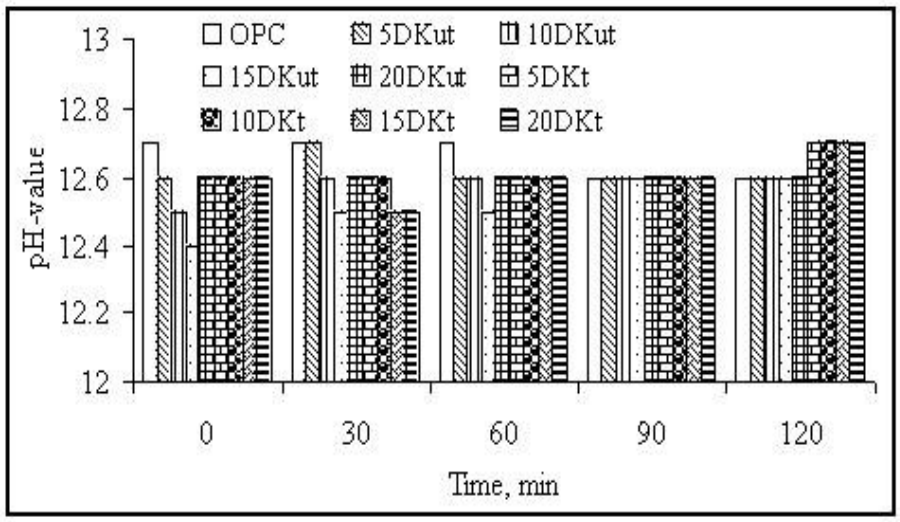

Figure 4.2 Effect of DK on pH value of cement slurry at different ages from mixing.

4.3.2 Setting Time

Figure 4.3 shows the effect of addition of both forms of DK (treated and untreated) on the water/binder ratio (w/b) ratio required for the standard consistency of the replaced OPC. It is clear from the figure that the w/b ratio increases with increasing the DK contents. The w/b ratios of DKut mixes are slightly higher than those of DKt for all replacement percentage.

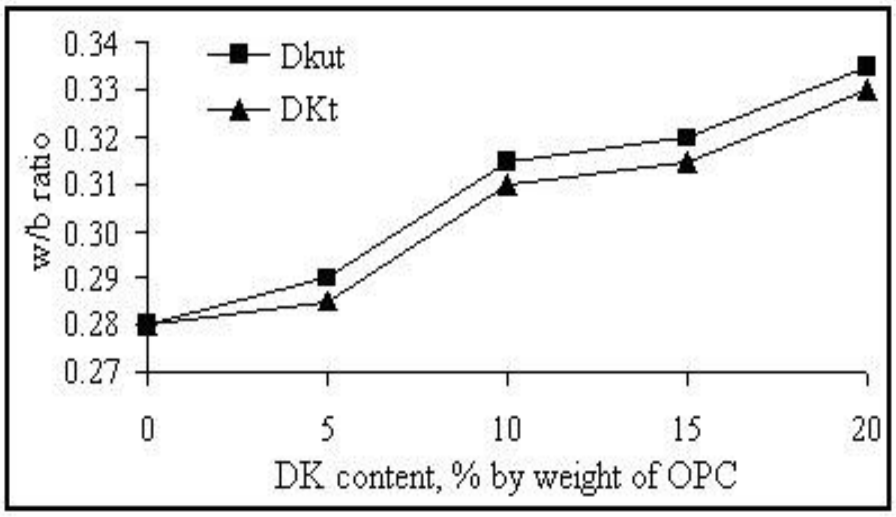

Figure 4.3 Effect of DK on the w/b ratio required for standard consistency of OPC paste.

Figure 4.4 shows the results of the initial and final setting times of the pastes with standard consistency containing the DKut and the DKt at different replacement of OPC. The setting times of the OPC paste without replacement was found to be around 120 and 160 minutes, respectively. The addition of 5% DKt leads to a slight decrease of both setting times and is

followed by a steady increase at higher replacement ratios up to 20%. In other words, the DKt has a slight accelerating effect at 5% replacement then acts as a retarder.

For the pastes containing the DKut, an opposite effect is produced: the initial and final setting time of OPC/DKut pastes decrease with the increase of DKut, i.e. the DKut behaves clearly as an accelerator. The accelerated effect of DKut appears to be significant on the initial setting time where about 25% reduction in the initial setting time was observed at a replacement ratio of 10%. The reduction in final setting time was only 18% at the same replacement percent. Generally the setting times for both DK pastes are within the recommended range for the OPC paste (initial setting time ≥ 45 minutes and final setting time ≤ 10 hours) according to ISO 9597 (1989) and ASTM C 305-82.

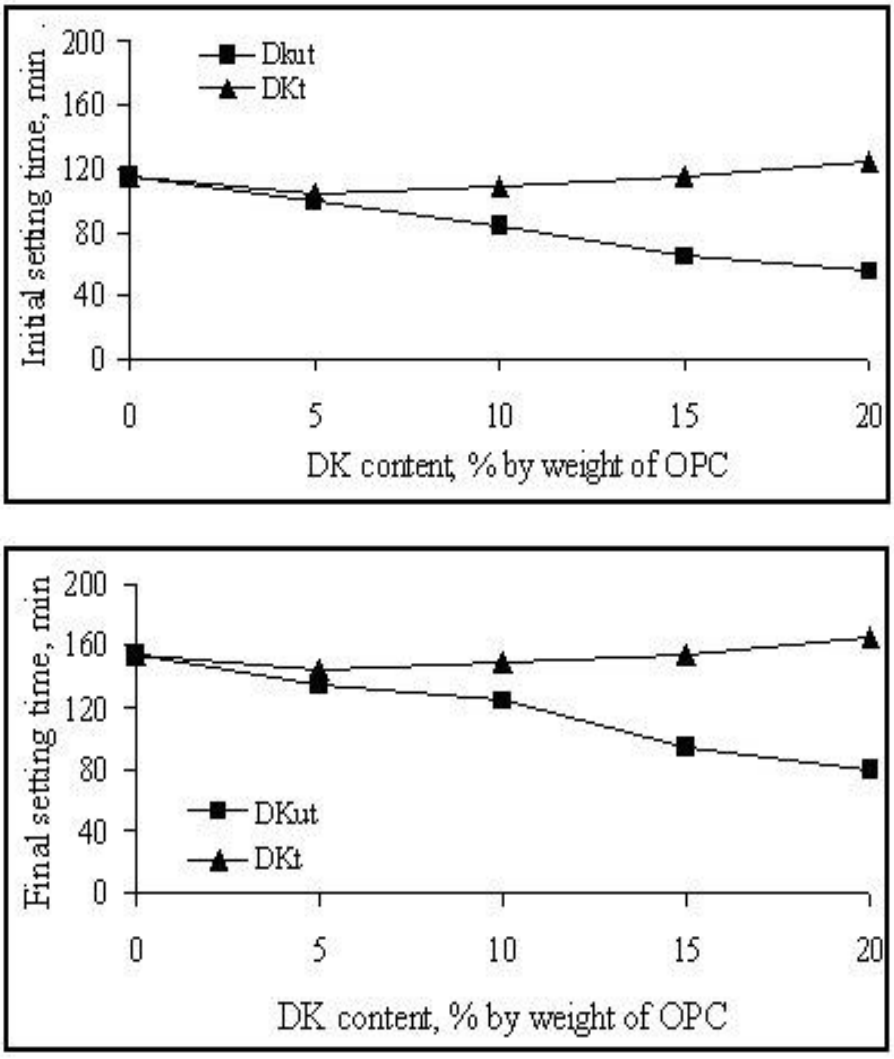

Figure 4.4 Effect of incorporating DK on OPC cement paste setting times.

4.3.3 Microstructural analysis

4.3.3.1 Thermal analysis

4.3.3.1.1 Differential Thermal Analysis (DTA)

The results obtained from the DTA of the 90 days hardened cement pastes prepared from OPC, OPC/DK mixes (5 and 10% replacement) and OPC/SF with 10% replacement are given in Figures 4.5 to 4.7. The thermal analyses being carried out up to a temperature of 1000°C. The figures show main endothermic effects at $\leq$150^{o}C which is quite diffuse and a clear one at 420-520ºC. The low endothermic effects may be attributed to the calcium sulfoaluminate hydrates as well as the CSH gel, while the higher temperature effect is related to portlandite. The portlandite peak of the OPC paste is seen to decrease significantly in the OPC/DKt and OPC/SF specimens, and with a lesser amount in the OPC/DKut.

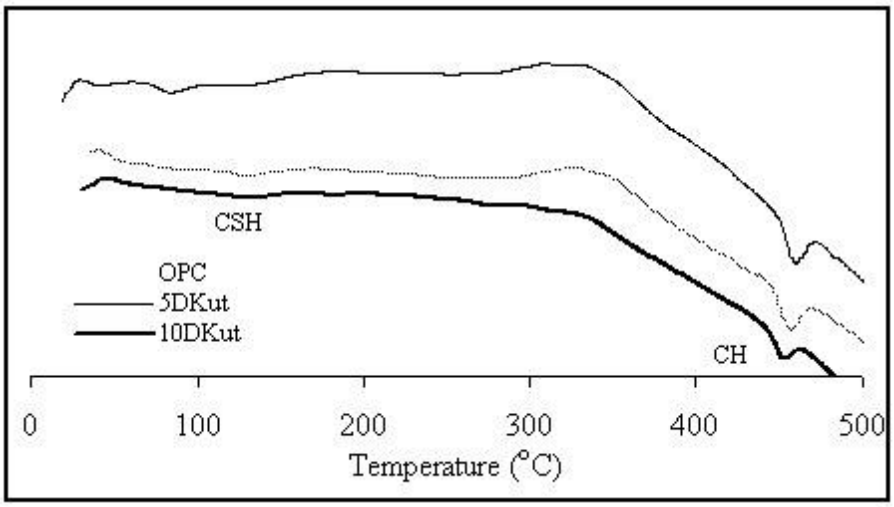

Figure 4.5 DTA Diagrams for OPC hardened cement pastes containing different content of DKut at age of 90 days.

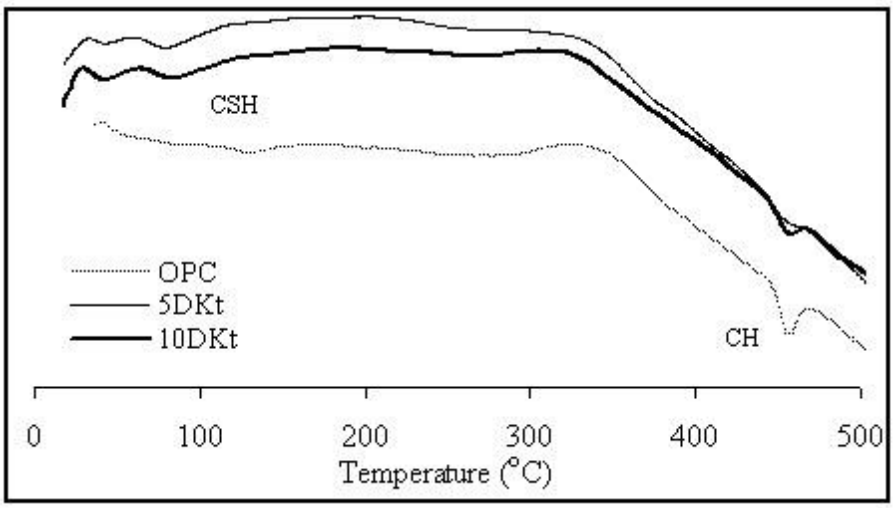

Figure 4.6 DTA Diagrams for OPC hardened cement pastes containing different content of DKt at age of 90 days.

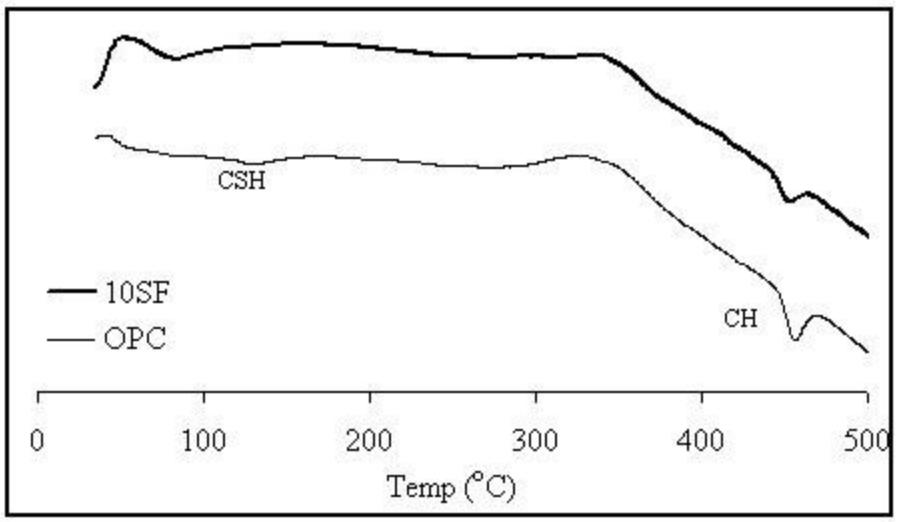

Figure 4.7 DTA Diagrams for OPC hardened cement pastes containing 10%SF at age of 90 days.

4.3.3.1.2 Thermogravimetric analysis (TGA)

The thermogravimetric method of analysis was used to evaluate a) the degree of hydration based on the amount of bound water, expressed in terms of Non-Evaporable Water content (% NEW). b) the amount of hydration products followed by Rahman and Glasser (1989) and Abdelaziz (1998) (see section 3.2.3.4.1). Worked examples for determination of NEW and phase composition of cement paste are reported in Appendix 2 and 3, respectively. Both systems are worked out through the evaluation of the weight change of the samples upon heating. The obtained results are illustrated in Figures 4.8 to 4.10.

a- Determination of the Non Evaporable Water content (NEW)

Figure 4.8 shows the percentage of bound water (NEW) measured for hardened cement pastes made of OPC as well as of Portland cement replaced partially by the DKut, DKt or SF after 90 days. The results indicates that the percentage of NEW increases by an maximum amount of 8% through 5 and 10% DK addition, the NEW is higher than that of OPC without replacement materials. The incorporating of 10% SF to the OPC mix increases the amount of bound water as well.

b- Determination of the CSH phases

Figure 4.9 indicates that the weight loss due to decomposition of CSH increases by a maximum of 15% in the presence of 5 and 10% DKut or DKt and by an amount of 20% as a result of incorporating 10% SF in the mix.

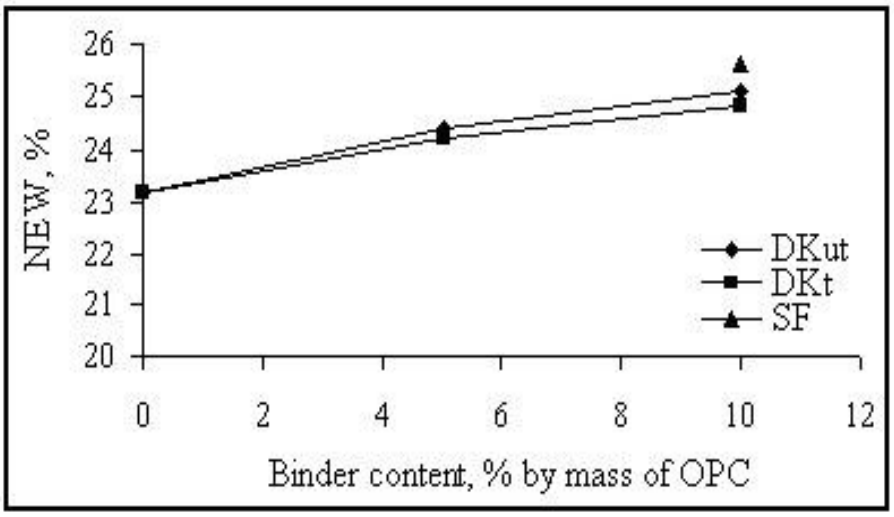

Figure 4.8 The non evaporable water content of hardened cement pastes made of OPC, OPC with 5 and 10% DK as well as of OPC with 10% SF; w/b = 0.5.

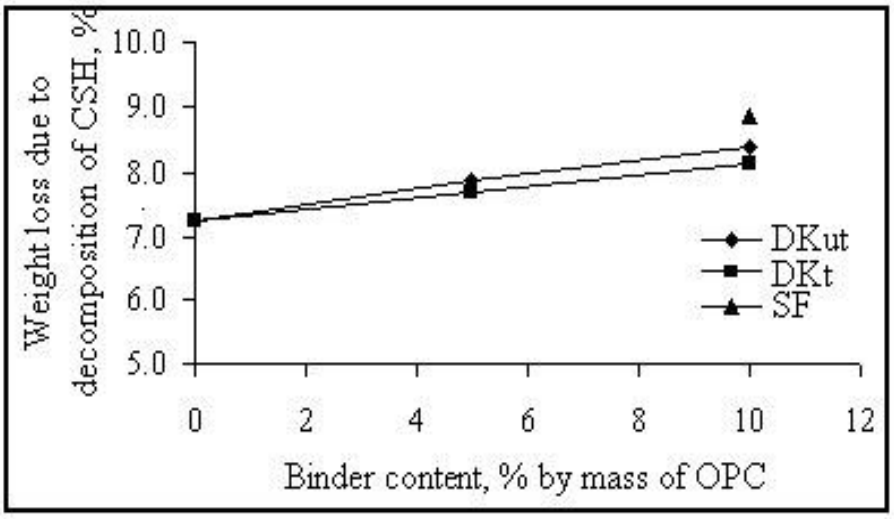

Figure 4.9 CSH of OPC hardened cement pastes incorporating different contents of DKut, DKt or 10%SF; w/b = 0.5.

c- Determination of portlandite

Figure 4.10 represents the weight loss due to decomposition of CH for different hardened OPC pastes made with either DKut or DKt contents of (0, 5 and 10%) or 10%SF. The figure shows that the amount of CH decreases by 13 and 32% with a partial replacement of the OPC by 5 and 10% DKut and by 10 and 27% with a partial replacement of OPC by 5 and 10% DKt. 65% decrease of CH occurs as a result of incorporating 10%SF in the OPC mix (Figure 4.10).

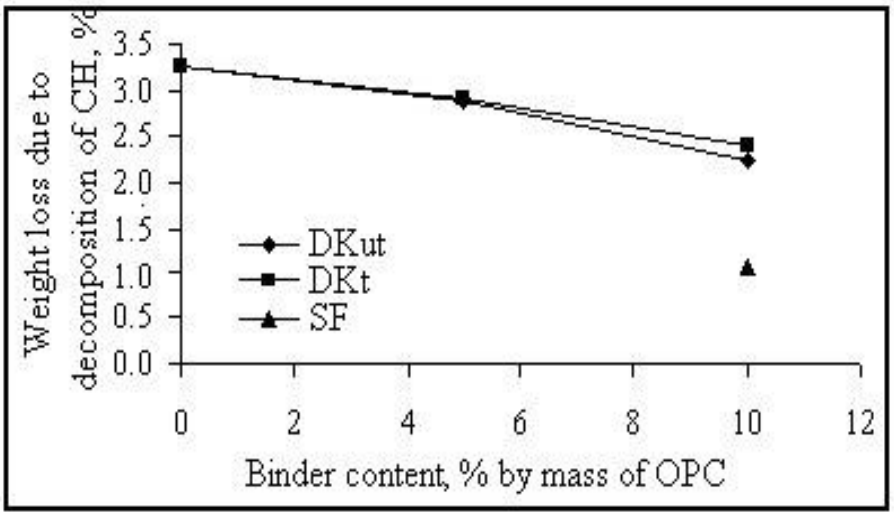

Figure 4.10 CH of OPC hardened cement pastes incorporating different contents of DKut or DKt or 10%SF, w/b = 0.5.

4.3.3.2 Phase analysis by means of X-ray diffraction

The X-rays diffraction patterns of the hardened cement pastes made of OPC, OPC/DK and OPC/SF are illustrated in Figures 4.11 to 4.13. It is clear from Figure 4.11 that the peaks characteristic of CH, CSH and unhydrated cement particles. The intensities of CH peaks decreased while, of CSH peaks increased with the amount of DKut. Moreover the Figure shows traces of C_2ASH_8 phase (weak peak at 31 (2θ)).

.

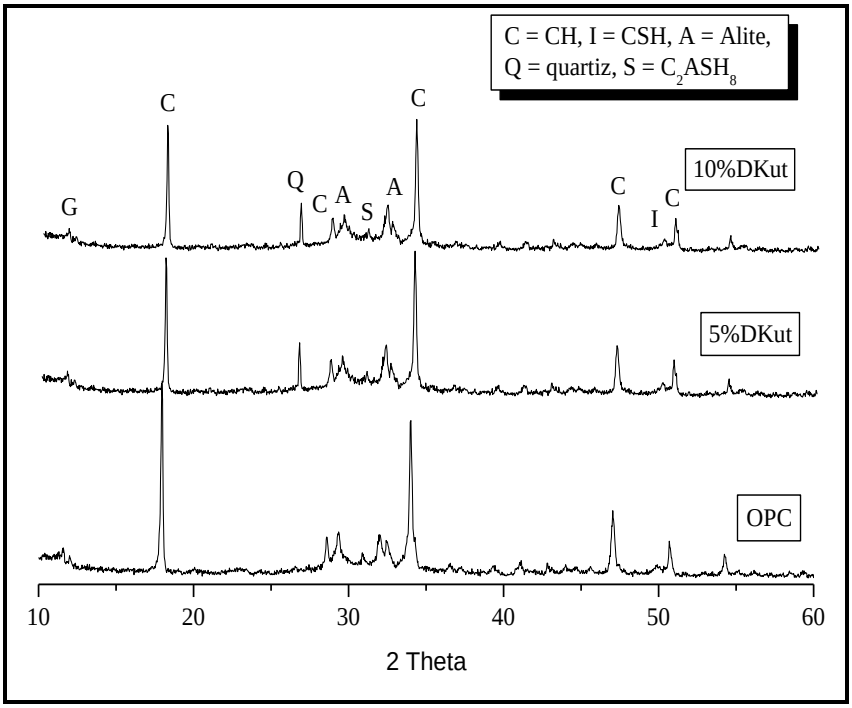

Figure 4.11 X-ray patterns for 90 days hardened cement pastes made of OPC as well as OPC/DKut.

Figure 4.12 shows the crystalline compounds of DKt-blended cements at 90 days. The results confirm that the behaviors of both DKut and DKt are similar. However, incorporating DKt in OPC mix decreases the CH peaks and increases the CSH and C_2ASH_8 peaks than DKut mixes.

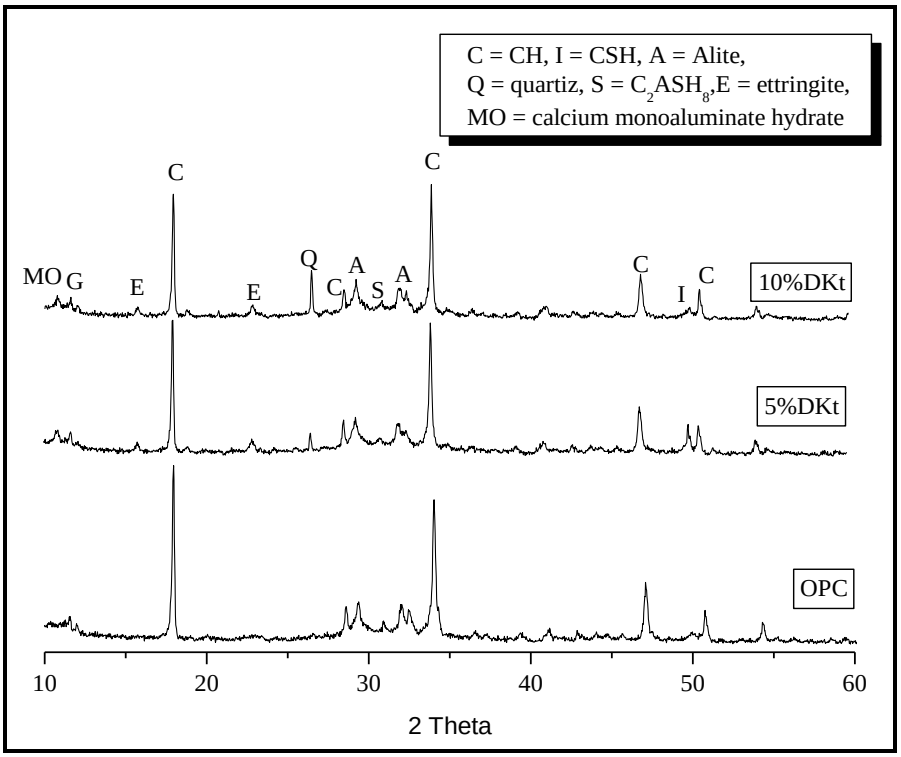

Figure 4.12 X-ray patterns for OPC hardened cement pastes containing different content of DKt at age of 90 days.

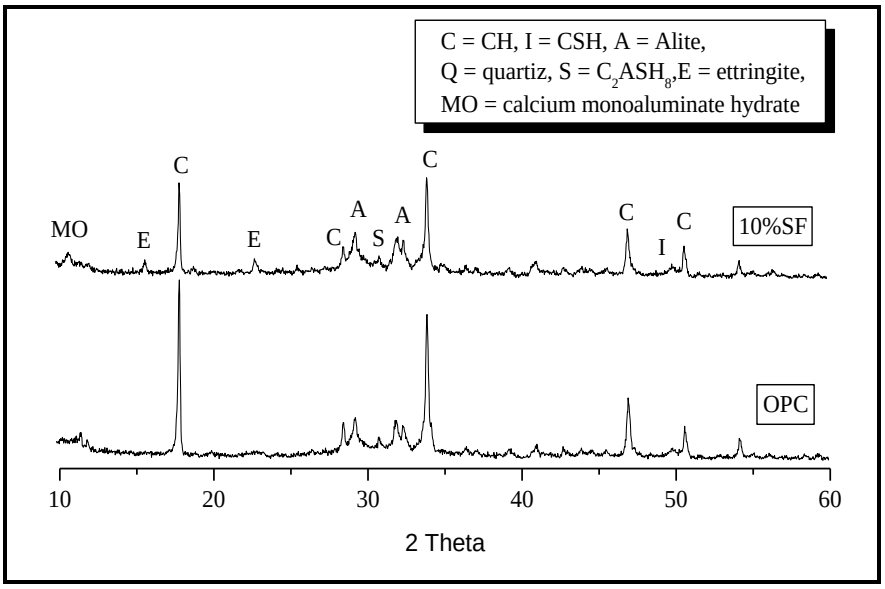

Figure 4.13 X-ray patterns for OPC hardened cement pastes containing 10%SF at age of 90 days.

Similarly for OPC/10%SF hardened cement paste, the peaks characteristic of CSH increased and that of CH decreased as a result of incorporating 10%SF in the OPC mix (see Figure 4.13). Comparing the patterns from samples containing DKut or DKt and that containing SF shows that, the peaks characteristic of CH for samples containing DKut or DKt is higher than the corresponding peaks of SF mixes. While, the peaks characteristic of CSH is found to be lower than the corresponding peaks of SF mixes.

The results obtained by X-ray diffraction (XRD) confirm the results of both thermogravemetric analysis (TGA) and differential thermal analysis (DTA). The results obtained by these techniques confirm that DK in its forms when incorporated in OPC matrix goes through a pozzolanic reaction with CH liberated from the hydration reaction of cement and forming CSH. As a consequence an increase in the amount of CSH and a reduction in the amount of CH were produced.

4.3.3.3 Morphology by means of Scanning Electron Microscope (SEM)

Figures 4.14, 4.15 and 4.16 show SEM images of the general feature of the glass-paste samples containing 0, 5 and 10%DKut by mass of OPC, respectively cured in water for 90 days. The glass piece shown in all Figures acts as aggregate particle (G). The Figures also, show the interfacial transition zone (ITZ) between the glass piece and OPC/DK paste and cement paste bulk zone (BZ).

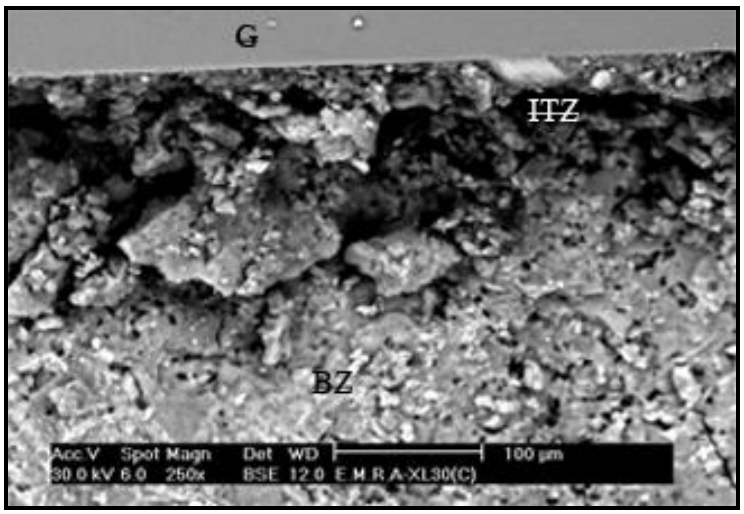

Figure 4.14 SEM micrograph of OPC paste specimen showing general features.

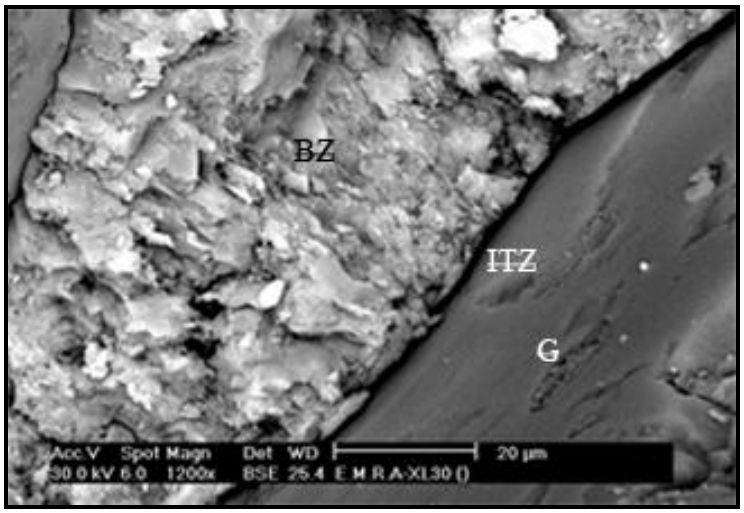

Figure 4.15 SEM micrograph of OPC/5DKut paste specimen showing general features.

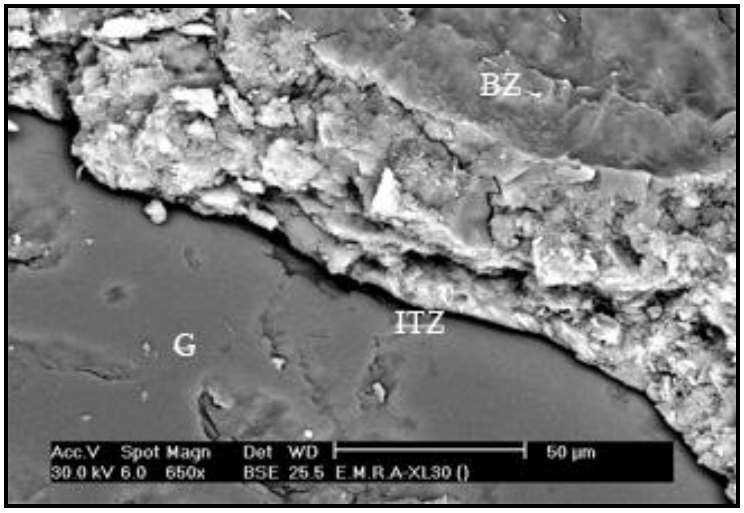

Figure 4.16 SEM micrograph of OPC/10DKut paste specimen showing general features.

4.3.3.3.1 Morphology of bulk paste zone

SEM micrographs and EDX spectrum of the bulk zone for the control cement paste (without DKut) is presented in Figures 4.17a and b. This image was taken as a window from the bulk zone of the glass-paste sample of the control specimen shown in the general view (Figure 4.14). SEM image 4.17b shows view of a window taken from Figure 4.17a at a higher magnification level 1500X. SEM images show the porous structure and presence of some microcracks in the OPC paste found at both low and high magnifications. It can also be found from the image of high magnification that CSH and a relatively significant amount of platy crystals of CH and some needle-like crystals typical of ettringite (E) were observed. The main elements found in the bulk zone of the control paste as given by EDX spectrum clarifies

that the main elements at the bulk zone of the control specimens are Ca, Si and traces of Al and Fe with % of 68, 22, 6, and 4. The ratio of Ca/Si was estimated and found to be 3.09.

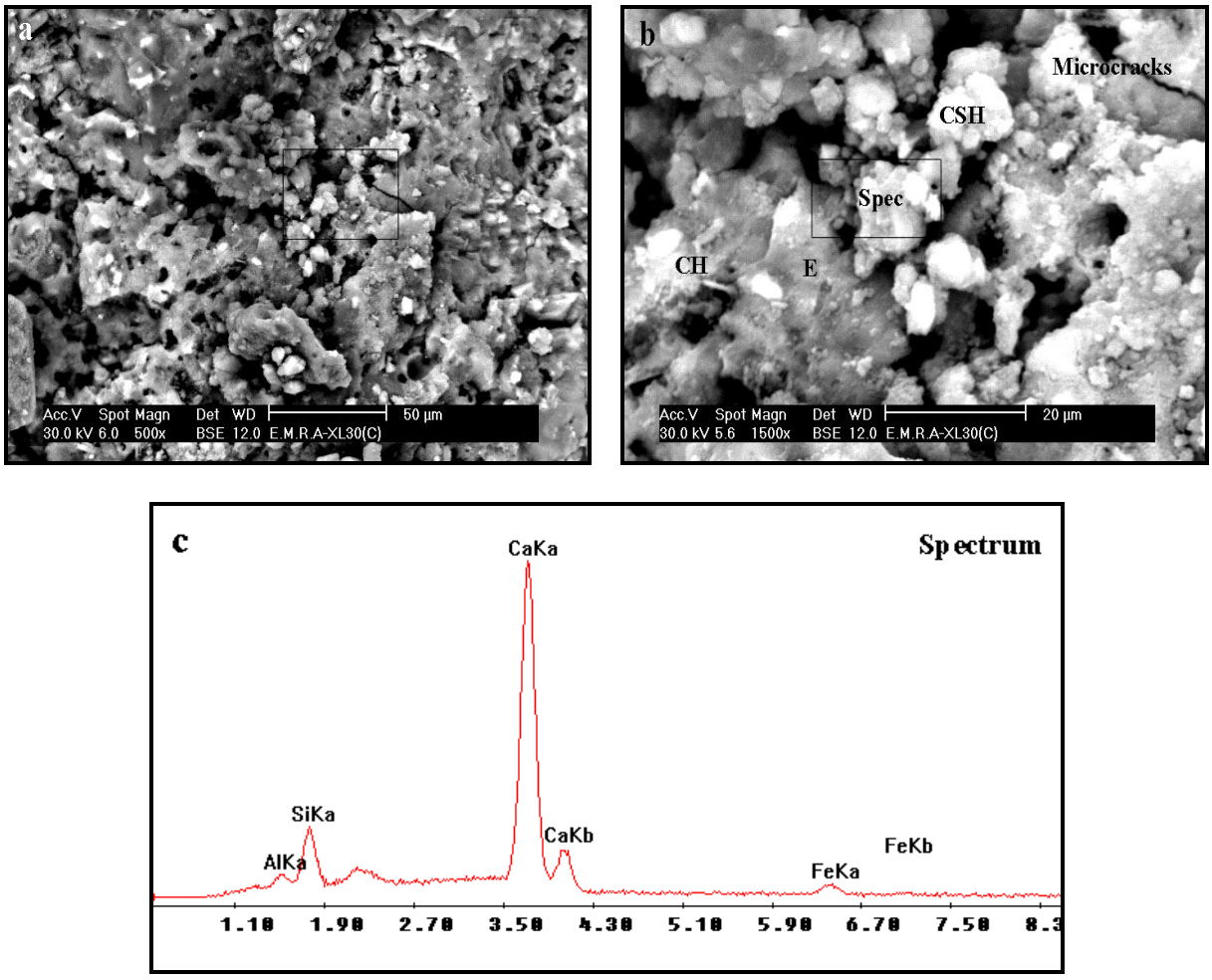

Figure 4.17 SEM image and EDX spectrum for OPC paste bulk zone.

Figure 4.18 shows the SEM micrographs and EDX spectrum of the bulk zone for hardened cement paste specimen containing 5%DKut. SEM images show a lower porous structure with fewer microcracks than that observed in the corresponding OPC bulk zone. It is also clear from SEM images that a lower amount of platy crystals of CH, a higher amount of CSH having a sponge-like morphology and slightly higher amount of ettringite of needle shape crystals than those in the corresponding control bulk zone. It can be concluded from EDX analysis that the main elements at the bulk zone of OPC/5%DKut paste sample are Ca, Si and traces of Al, Fe and S with % of 59, 32, 5, 2 and 2%. The ratio of Ca/Si was found to be 1.84, which is lower than that of OPC bulk zone.

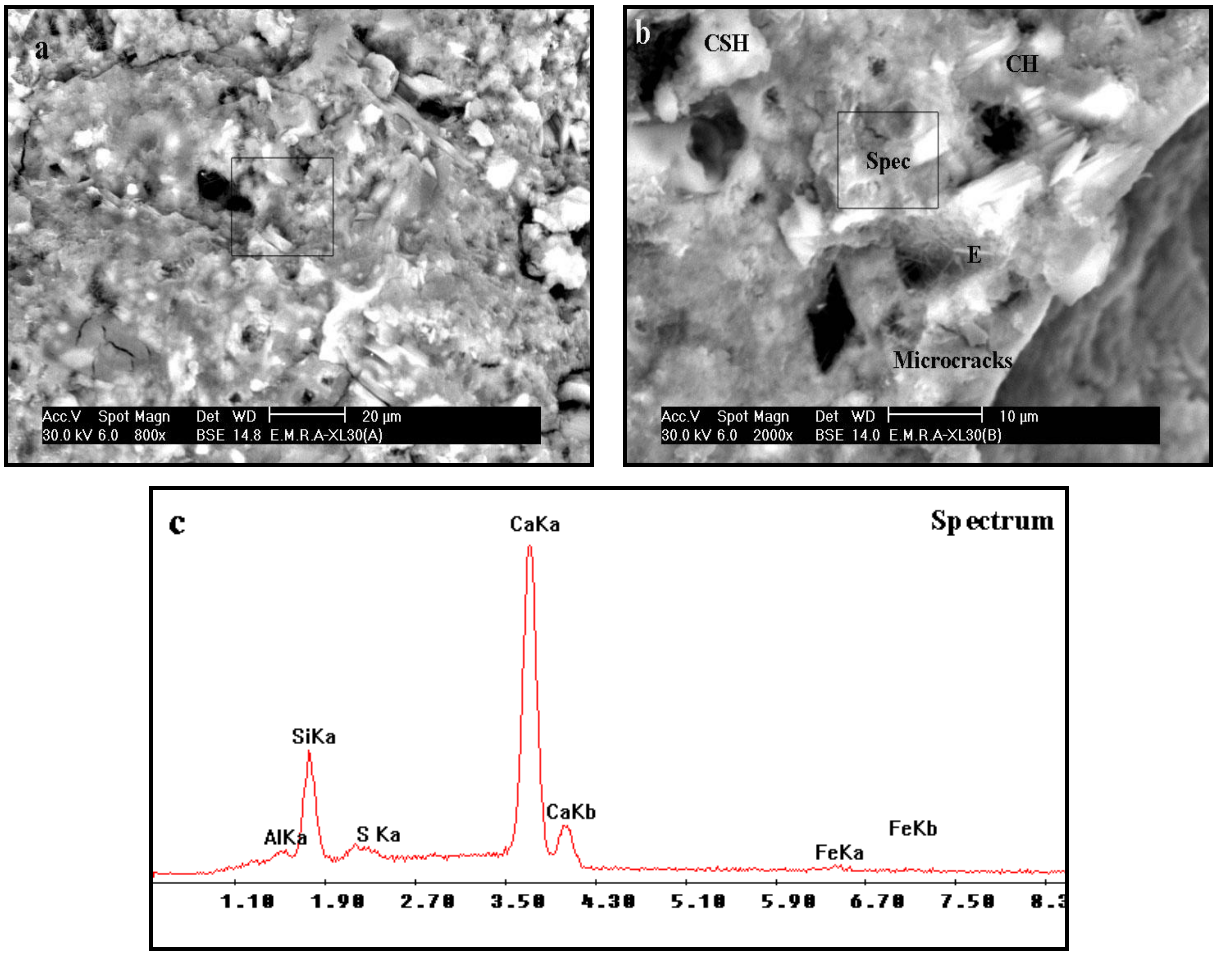

Figure 4.18 SEM image and EDX spectrum for OPC/5DKut paste bulk zone.

The bulk zone of the hardened cement paste specimen containing 10%DKut was examined. SEM images and EDX spectrum are shown in Figure 4.19. SEM images show a more dense structure with the presence of some microcracks. The images also shows a decreased amount of platy crystals of CH and a higher amount of CSH having a sponge-like morphology as well as a higher amount of needle-like crystals typical of ettringite are presented. EDX spectrum analysis shows that main elements at the bulk zone are Ca, Si, Fe and traces of Al, Ti, and K with % of 33, 26, 28, 6, 1, and 2. The ratio of Ca/Si was estimated and found to be 1.27.

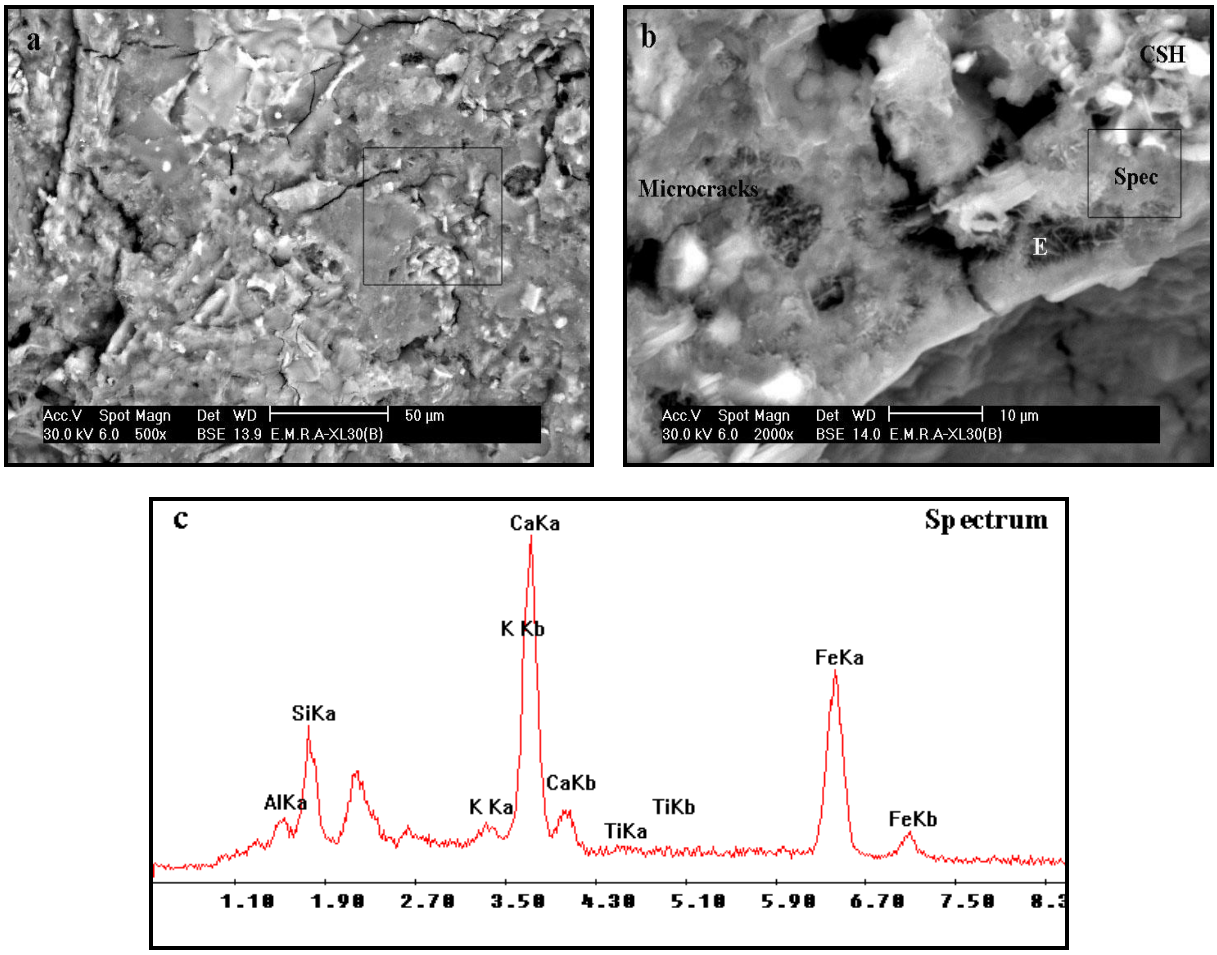

Figure 4.19 SEM image and EDX spectrum for OPC/10%DKut paste bulk zone.

4.3.3.3.2 Microstructure of interface with glass

Figure 4.20 shows the SEM micrograph and EDX spectrum of OPC paste at the interface near the glass of the control paste specimen. This image was taken as a window magnified to 3500X at the interface of the glass-paste sample of the control paste shown in the general view (Figure 4.14). SEM image shows the weak structure of the interfacial transition zone with decreased CSH and a relatively significant amount of platy crystals of CH were observed. The EDX spectrum shows that the main elements at the interface of the control paste compose of Ca, Si and traces of Al and Fe with % of 71, 19, 5, and 5. The ratio of Ca/Si was estimated and found to be 3.73, which is higher than that of the bulk paste.

The ITZ of the hardened OPC/5%DKut cement paste specimen was examined. SEM images and EDX spectrum are shown in Figure 4.21. The Figure shows a less porous structure than that observed in the corresponding OPC specimen ITZ with lower amount of CH and higher amount of CSH. EDX spectrum analysis clarifies that main elements at the interface are Ca,

Si and traces of Al and S with the % of 70, 25, 4, and 1. The ratio of Ca/Si was estimated and found to be 2.8.

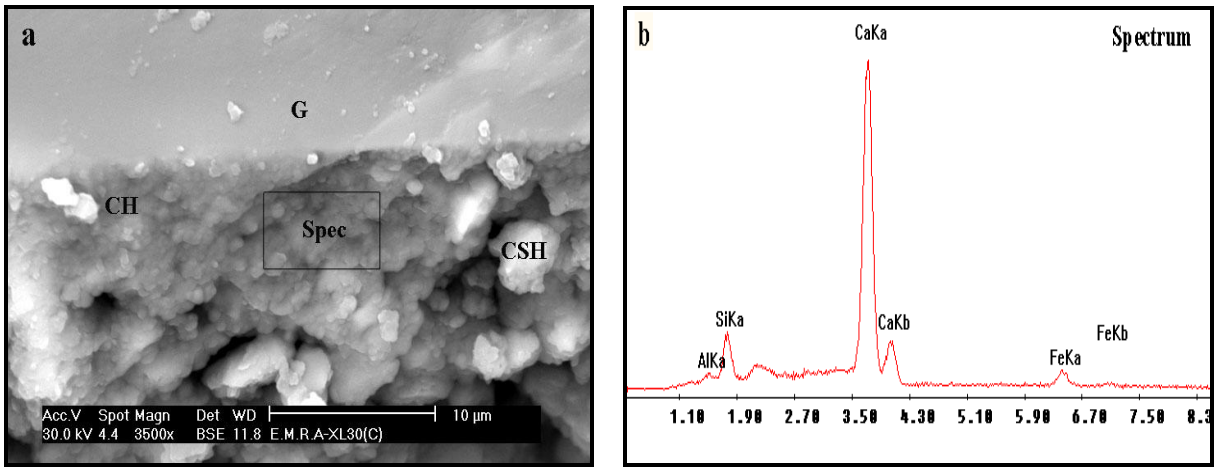

Figure 4.20 SEM image and EDX spectrum for OPC paste specimen showing interfacial zone.

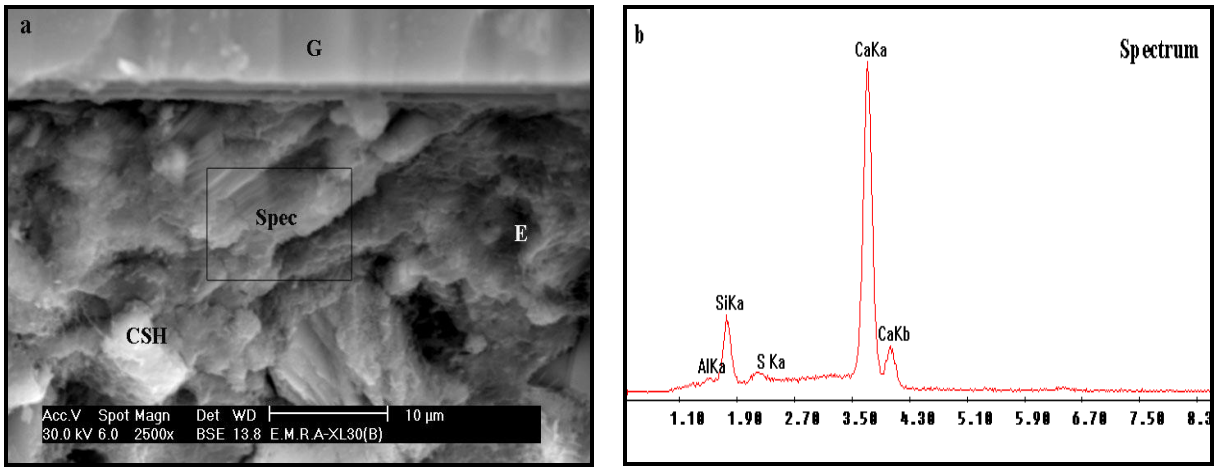

Figure 4.21 SEM image and EDX spectrum for OPC/5%DKut paste specimen showing interfacial zone.

SEM micrographs and EDX spectrum of the ITZ for paste containing 10%DKut is presented in Figures 4.22. The Figure shows no CH and a higher amount of less dense CSH having a sponge-like morphology as well as some needle-like crystals typical of ettringite are present. The main elements at this interface as given by X-ray spectrum analysis are Ca, Si and traces of Al, Fe Ti, and K with % of 54, 28, 7, 7, 1, and 2. The estimated Ca/Si ratio was found to be 1.93.

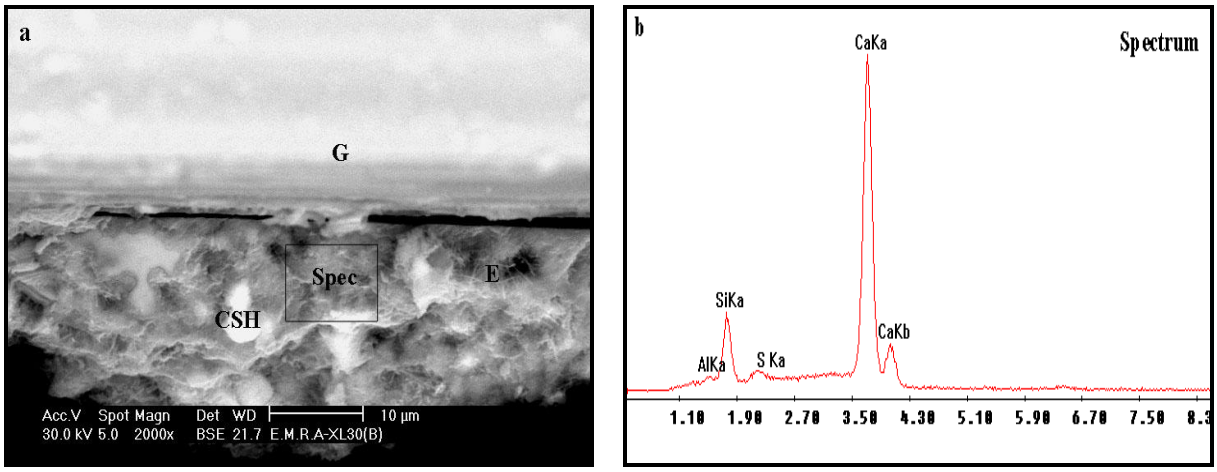

Figure 4.22 SEM image and EDX spectrum for OPC/10%DKut paste specimen showing interfacial zone.

The comparison of Ca/Si ratio between the three cases of cement paste samples without and with 5 and 10%DKut is shown in Figure 4.23. The results indicate that the incorporation of DKut to the cement matrix can lead to decrease Ca/Si ratio for both aggregate-paste ITZ and bulk zone and the amount of reduction increases with the amount of DKut.

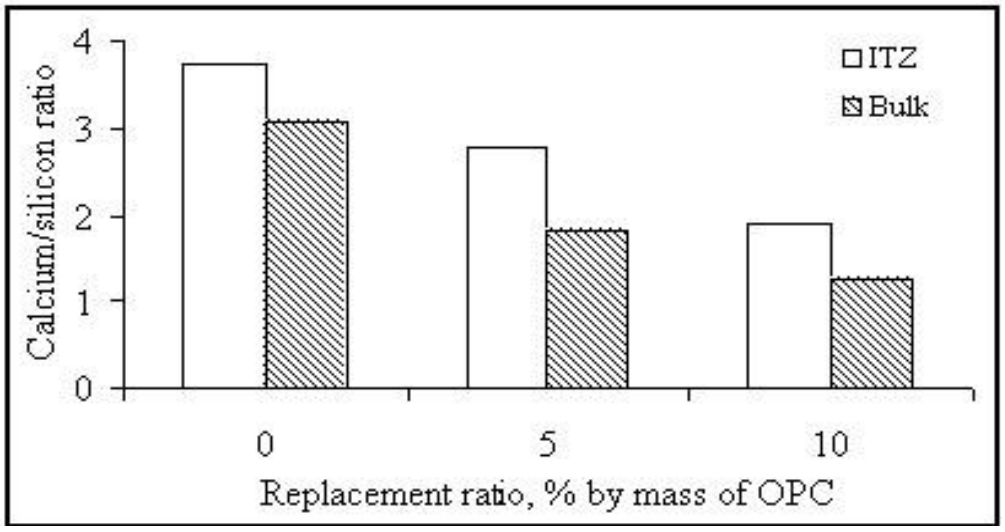

Figure 4.23 Effect of DKut content on the ratio of calcium to silica for hardened cement paste samples at age of 90 days.

4.3.4 Pore structure

4.3.4.1 Porosity by desorption test

The desorption technique was adopted in this study to obtain comparative results for the pore structure of OPC/DK hardened cement paste. A worked example for determination of the total and capillary porosity is explained in Appendix 1. In order to have a more reliable and accurate results for pore structure and pore size distribution (PSD) for OPC/DKut paste,

samples containing different content of DKut (0, 5, and 10% by mass of OPC) were tested using mercury intrusion porsometery (MIP) test.

a- Total porosity

The total porosity derived from the desorption test results for different OPC hardened cement paste containing various contents of either DK two forms or SF, (0, 5 and 10%) made with constant w/b ratio of 0.5 and cured in water for 90 days, are shown in Figure 4.24. It can be seen that the total porosity of OPC/DKut specimens was not affected or slightly increased as a result of inclusion of DKut and the amount of increase increases with increasing DKut content. The amount of increase reaches 3 and 5 %, when 5 and 10% DKut were used, respectively. Similar results were observed for DKt mixes. For OPC hardened cement paste incorporating different contents of SF, similar trends were obtained (see Figure 4.24). The amount of increase in total porosity for OPC specimens containing SF content of 5 and 10% reaches 4 and 8%, compared to that of OPC specimens.

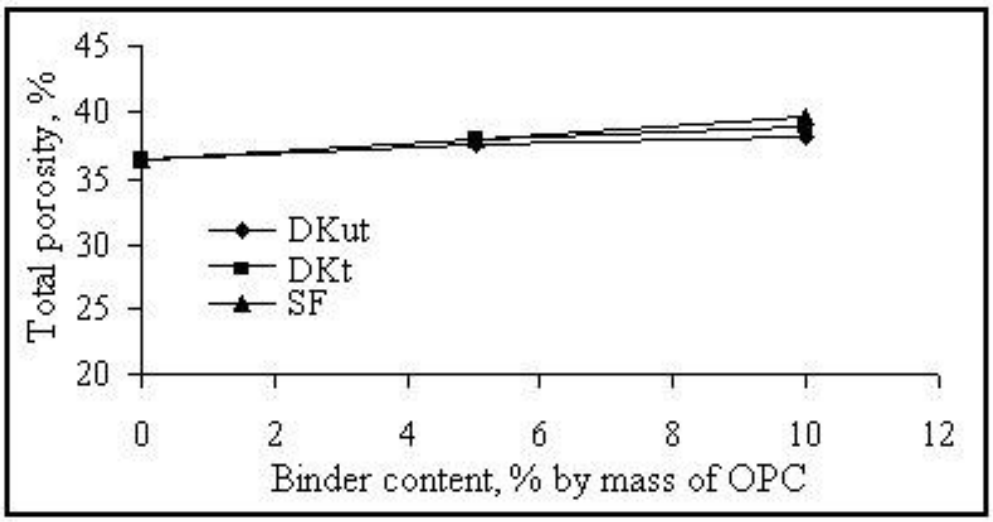

Figure 4.24 Total porosity of OPC hardened cement pastes made with different contents of either DKut, DKt or SF; w/b = 0.5.

b- Capillary porosity

The capillary porosity for different OPC hardened cement paste containing various contents of either DK two forms or SF, made with 0.5 w/b ratio and cured in water for 90 days, are illustrated in Figure 4.25. It is clear that the capillary porosity of OPC/DKut specimens decreased as a result of incorporation of DKut. The amount of reduction in the capillary porosity increased with increasing DKut content, where it reaches 12 and 15%, when 5 and

10% DKut were used, respectively. Similar results were observed for the capillary porosity of DKt mixes but the amount of reduction was less than that of DKut mixes.

It is clear that the capillary porosity of OPC/SF specimens is significantly decreased as a result of inclusion of SF in the matrix and the amount of reduction reached 20 and 38%, when 5 and 10% SF content were utilized, respectively. The capillary porosity of OPC/SF specimens was, less than the corresponding OPC/DKut.

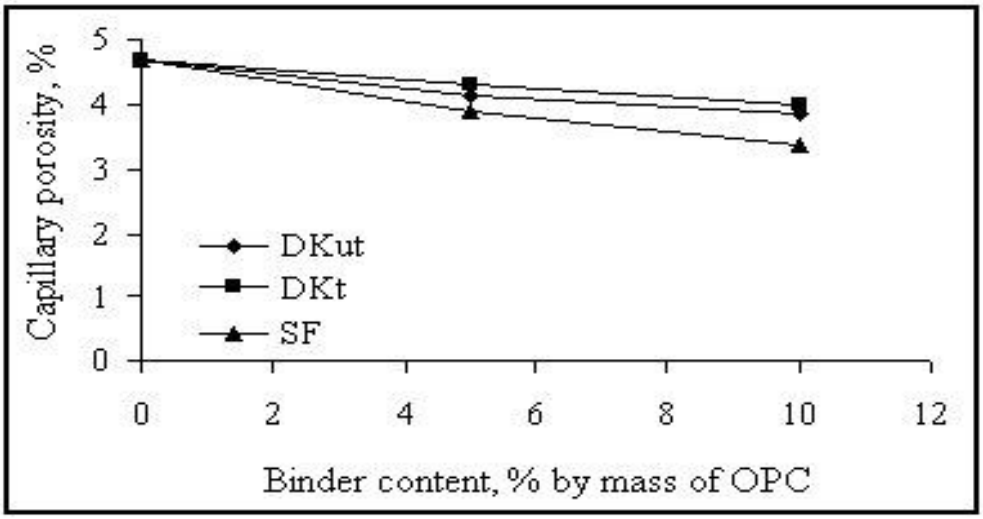

Figure 4.25 Capillary porosity of OPC hardened cement pastes made with different contents of either DKut or DKt or SF; w/b = 0.5.

4.3.4.2 Porosity and pore size distribution by Mercury Intrusion Porosimetry

4.3.4.2.1 Porosity

The total, capillary (pore diameter ≥ 30 nm) and gel (pore diameter ≤ 10 nm) porosities of HCP containing various contents of DKut (0, 5, and 10% by mass of OPC) shown in Figure 4.26 were deduced from the PSD curve shown in Figure 4.25. It can be seen from these results that the total porosity slightly increases or almost not changed by DKut addition. However, the effect of DKut incorporation is more pronounced for the capillary porosity than for the total porosity. The values of the total porosity of all examined mixes obtained between 29-30%, whilst the amount of reduction in capillary porosity reaches approximately 5 and 9% when DKut content were increased from 5 to 10% respectively. On the other hand, the gel porosity increases with increasing DKut content. The amount of this increase reaches about 6 and 10% for 5 and 10% DKut were used respectively, compared to the corresponding amounts of pure OPC paste specimens.

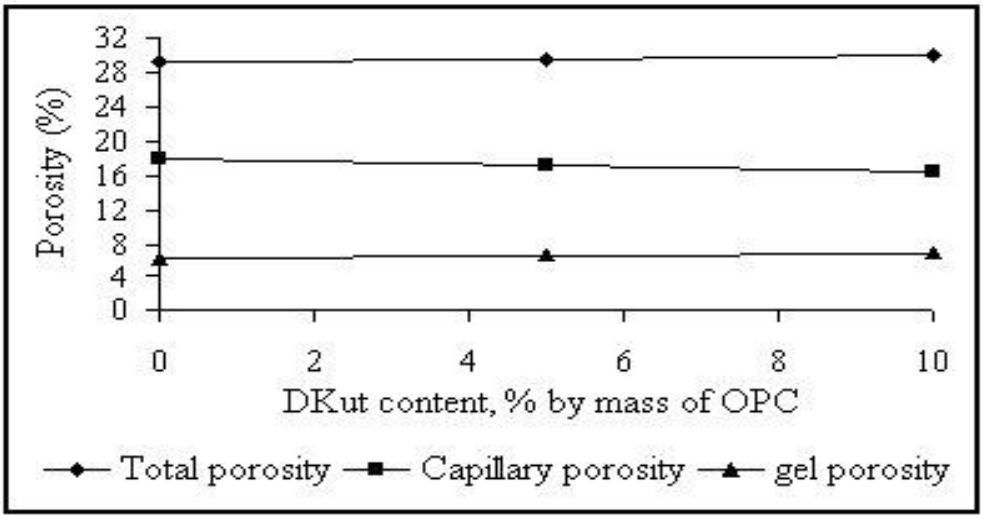

Figure 4.26 Total, capillary and gel porosity of OPC pastes containing 0, 5 and 10%DKut.

4.3.4.2.2 Pore size distribution

The effect of DKut incorporation as a partial cement replacement material on the PSD of OPC paste matrix was studied using MIP technique. The results are represented in Figure 4.27. It can be seen that the PSD of OPC paste is not influenced by DKut incorporation.

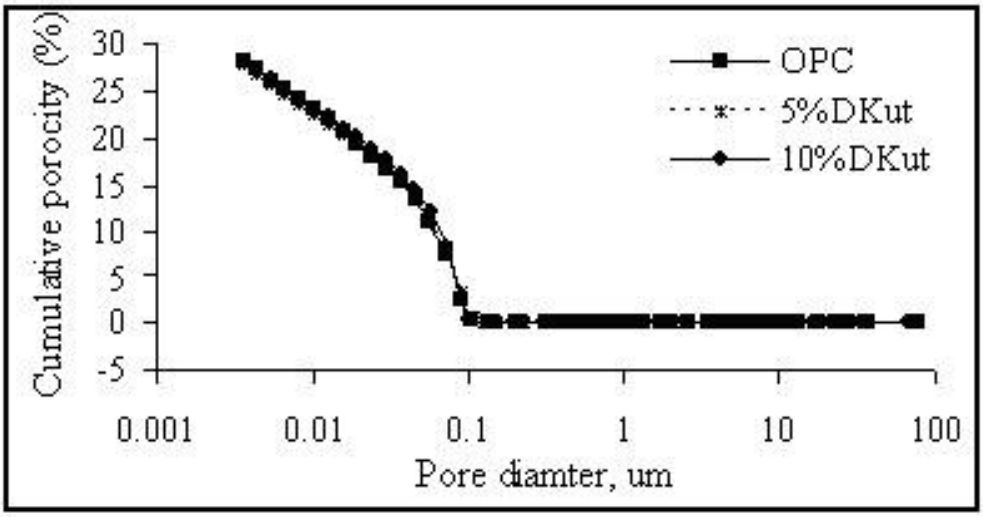

Figure 4.27 Pore size distributions of OPC pastes containing 0, 5 and 10%DKut.

4.4 MORTARS

4.4.1 Fresh Properties

The properties measured for the fresh mortars are the flowability, flowability loss and rheology. The results obtained are described below.

4.4.1.1 Flowability

The variation in the initial flowability of the OPC mortar as a result of cement replacement by DKut, DKt and SF is shown in Figure 6.28. The results indicate that the flowability of the OPC mortar is only slightly affected by the DKut but is significantly reduced with increasing the amount of the DKt and SF. The maximum depression attained by 20% replacement materials is 5, 20 and 30% for the DKut, DKt and SF respectively. At constant replacement of the dealuminated kaolin, the initial flowability of the mortars is higher than that in the presence of SF.

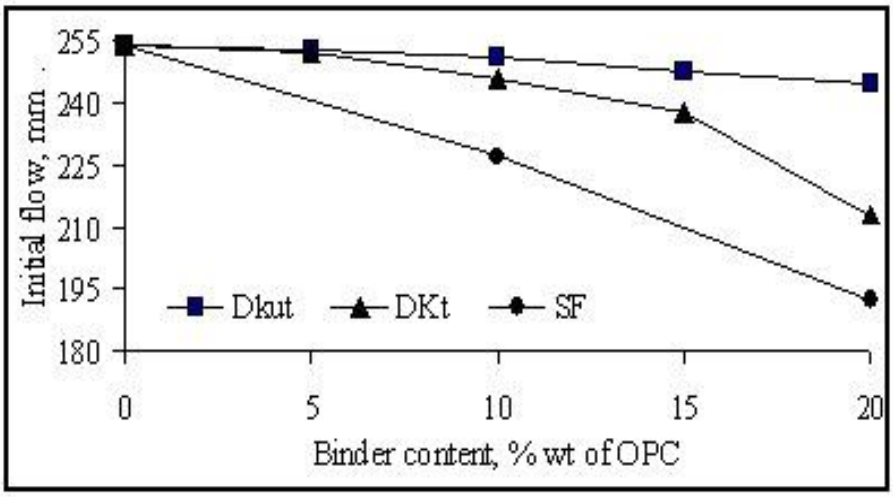

Figure 4.28 Flowability of OPC mortar containing different contents of DKut, DKt and SF.

4.4.1.2 Flowability loss

The results obtained from measuring the rate of instantaneous flowability loss at different elapsed periods of the mortars made of OPC, OPC/DK or OPC/SF is presented in Figure 6.29 (a-c). In the figure the values of the relative flowability (% of instant flowability to initial flowability) are plotted against EP. The figure shows that the relative flowability decreases with increasing EP for all mortars investigated. The effect is pronounced with increasing both types of the dealuminated kaolin (DKut, DKt) content. The rate of flowability loss is higher in the OPC/DKut mixes compared to those of the DKt at all replacement levels. The flowability loss of the OPC mortar is less affected by SF compared to the DK and does not undergo a remarkable change with the increase of the SF content in the cement matrix At 10% replacement of OPC by DK or SF, the values of relative flowability attained after 90 minutes from mixing are around 60 and 78% of the initial value in the presence of the DKut and DKt respectively, and 83% for the system with SF.

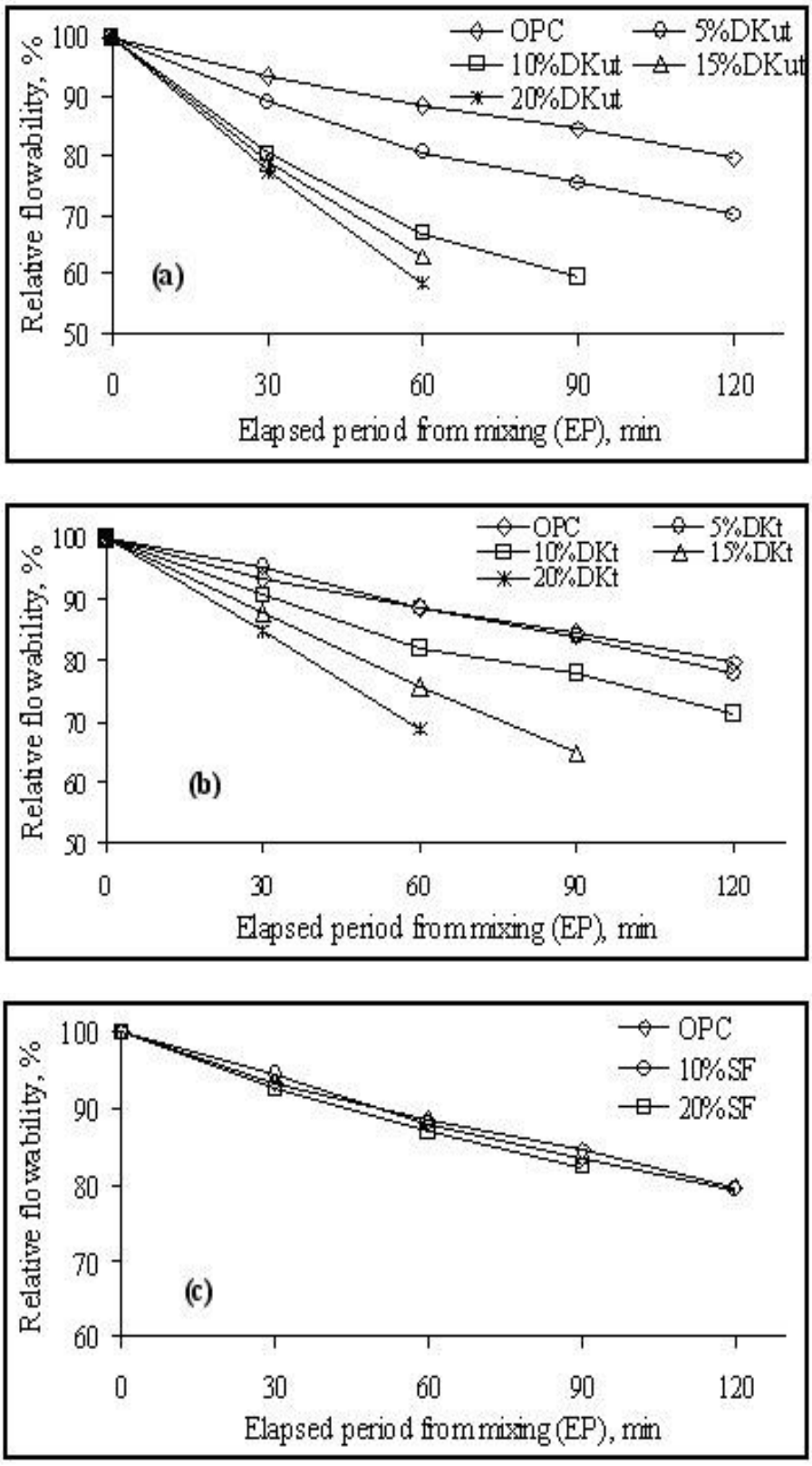

Figure 4.29 Flowability loss of OPC mortars containing different contents of a) DKut, b) DKt and c) SF.

4.4.1.3 Rheology

The relationship between the number of blows and the corresponding instant flowability of various OPC mortar mixes containing DKut and DKt contents of 5 and 10%, as cement replacement material at different elapsed periods (EP) from mixing are illustrated in Figures 4.30 (a-c) and 4.31 (a-c).

The results show that at EP = 0, a direct proportional correlation exists between the number of blows applied and the flowability of OPC and OPC/DKut mixes The correlation seems to be similar to that of OPC mix, where no change is observed in the correlation factor (R^2). The linearity of the correlation increases with increasing the amount of DKt in the OPC mix, in this system the correlation factor (R^2) is found to be equal to 0.85, 0.88 and 0.91 at 0, 5 and 10% DKt respectively, as shown in Table 4.5.

At EP = 0 the initial flowability which corresponds to the no. of blows = 0, also the instant flowability decrease slightly with increasing the DK content in the OPC mix. The reduction is more pronounced at longer elapse time of EP = 40 and 90 min as well as in the presence of DKut. At EP of 90 min, the initial and instant flowability for the mix with 10%DKut could not be measured because the mix had already set (see Figure 4.4). However, the positive effect of the DKt on the rheological properties of OPC mixes diminishes with increasing the elapse time: the (R^2) values were found to be 0.925, 0.936 and 0.965 at EP= 40 min, and 0.948, 0.955 and 0.965 at EP= 90 min for the OPC mortar and OPC with 5 and 10% replacement with DKt.

The slopes of the trend lines (Θ) shown in Figures 4.30, 4.31 are evaluated and listed in Table 4.5. For OPC/DK mortar mixes the value of (Θ) is found to decrease with increasing the DK content. The average values are 5.69, ~5.50 and ~5.42 for the OPC mortars as well as OPC with 5 and 10% both types of DK at EP = 0. Table 4.4 shows that the value of (Θ) decreases with increasing the elapse time (EP).

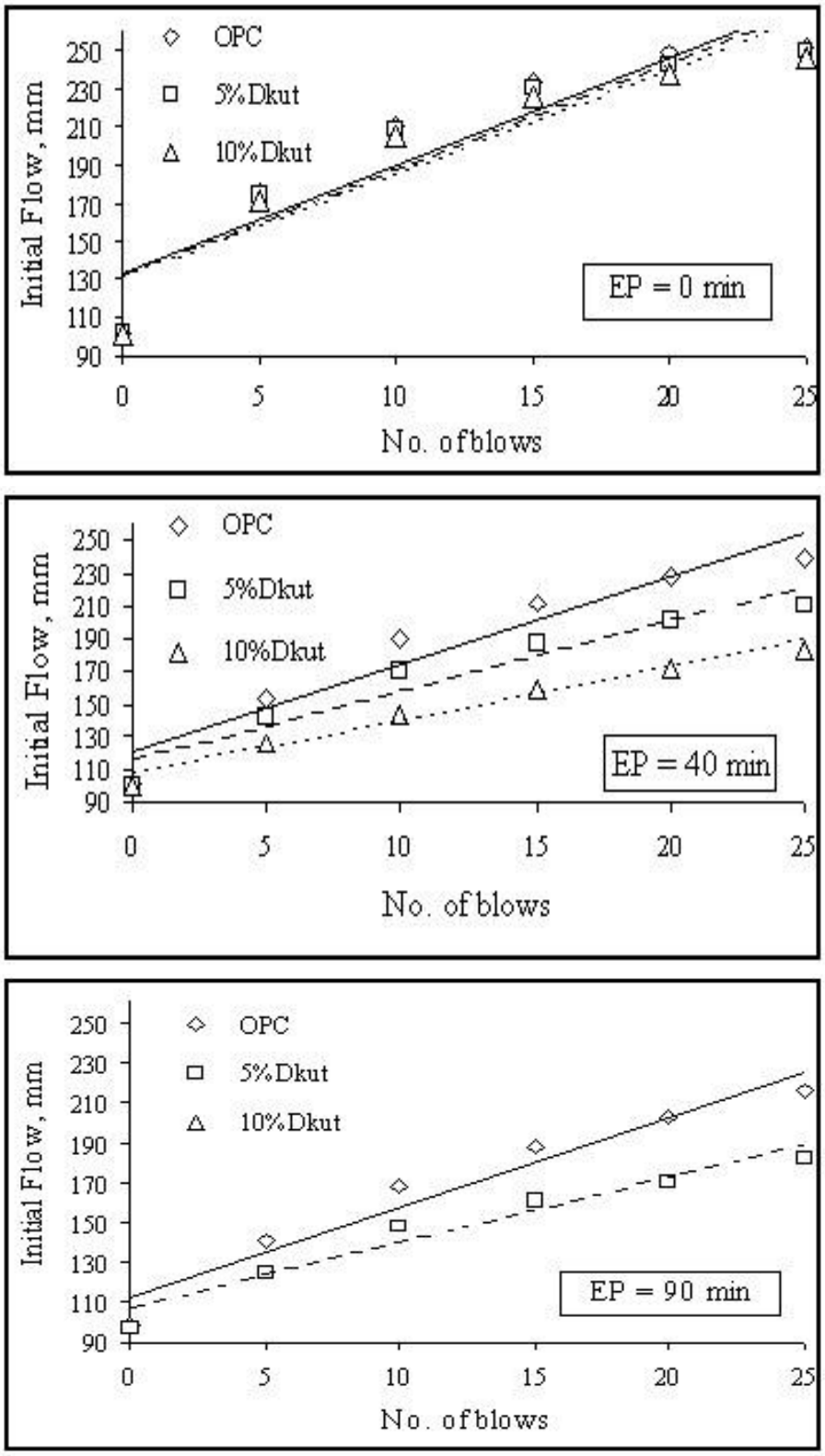

Figure 4.30 Flowability of OPC mortar containing different contents of DKut versus the external applied stress (No. of blows) at different elapsed periods (EP) from mixing.

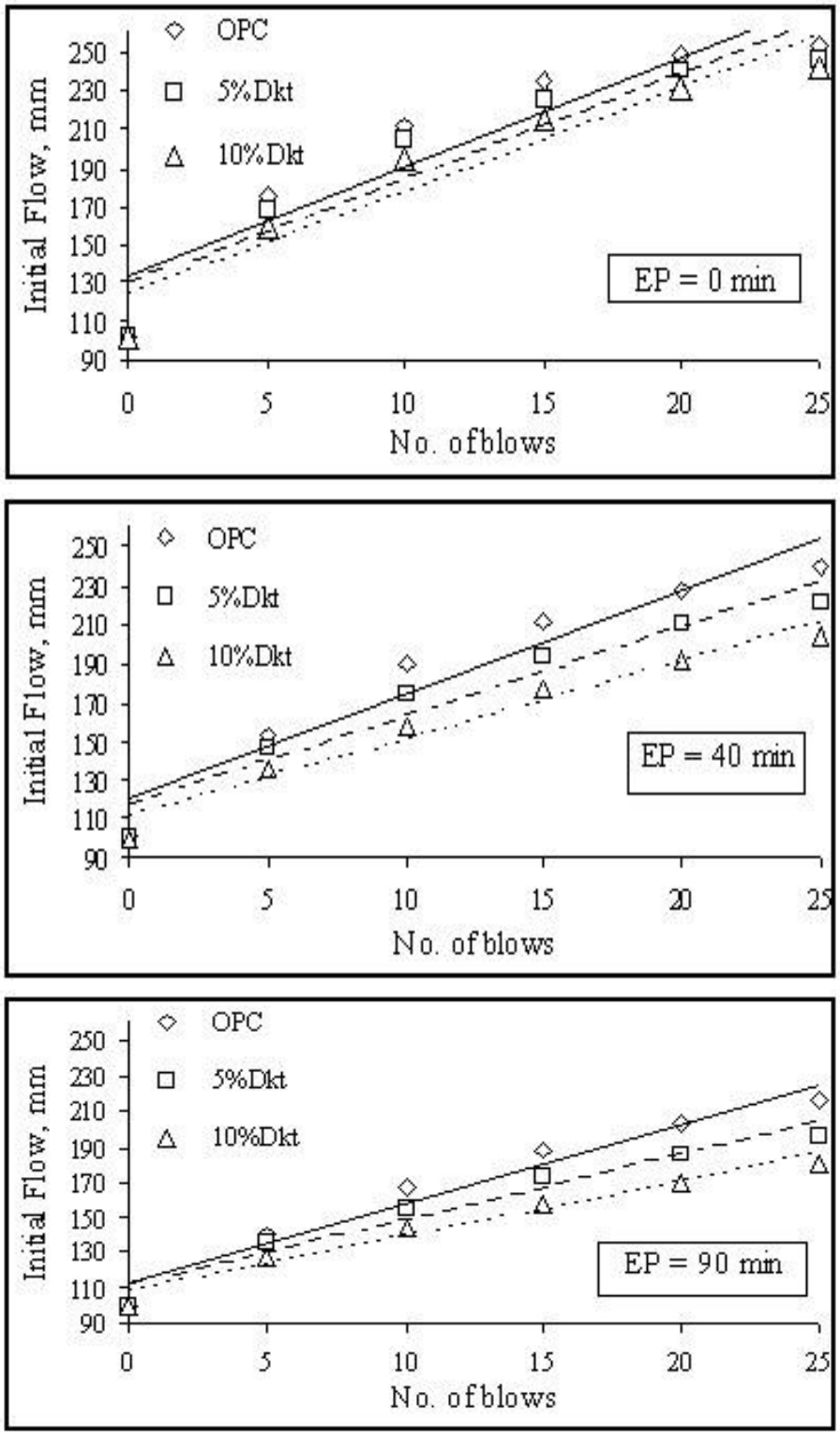

Figure 4.31 Flowability of OPC mortar containing different contents of DKt versus the external applied stress (No. of blows) at different elapsed periods (EP) from mixing.

Table 4.5 Correlation factor (R^2) and the slop of trend lines (θ) of the plotted relationship between applied stress (No of blows) and flowability of OPC, OPC/DKut and OPC/DKt mortar at different elapsed periods from mixing (EP)

Mix No.	Mix code	Slop of trend lines, (θ)			Correlation factor (R^2)		
		Elapsed period (min)					
		EP= 0	EP=40	EP=90	EP=0	EP=40	EP=90
1	OPC	5.69	5.36	4.53	0.855	0.925	0.948
2	95%OPC/5%DKut	5.52	4.25	3.29	0.856	0.928	0.952
3	90%OPC/10%DKut	5.42	3.27	----	0.862	0.972	----
4	95%OPC/5%DKt	5.45	4.61	3.7	0.873	0.936	0.955
5	90%OPC/10%DKt	5.38	4.06	3.13	0.911	0.965	0.965

4.4.2 Mechanical Properties

4.4.2.1 Compressive strength

Figure 4.32 illustrates the effect of replacing the OPC by DK and SF on the compressive strength of mortar specimens cured for 56 days in water. It is clear from the figure that the strength of the OPC mortar increases steadily with increasing the SF content, the strength of the OPC/DK mix, however, increases up to 10% replacement ratio then declines. The SF-curve lays higher than those of the OPC/DK mix. The individual values of the DKut are slightly better than the strength of the DKt.

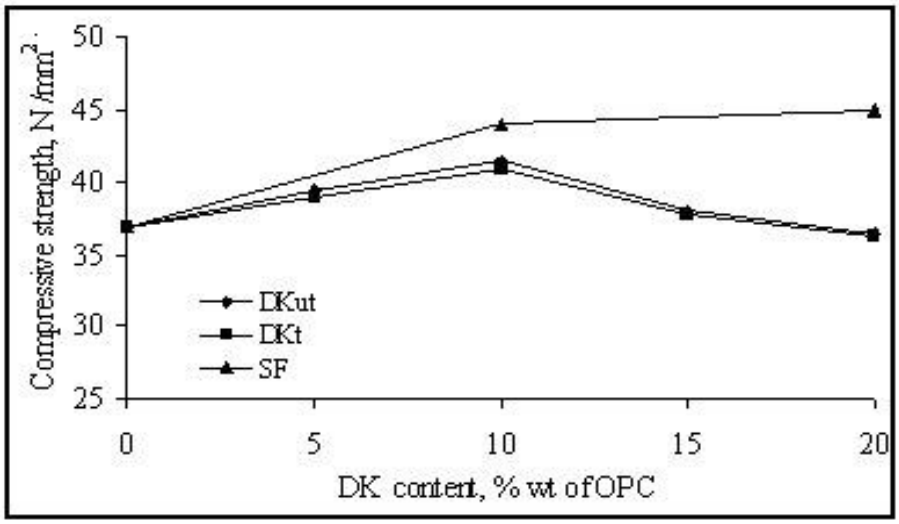

Figure 4.32 Effect of binder type (DKut or DKt or SF) and content on 56-day compressive strength of OPC mortar.

The effect of curing time on the compressive strength of the mortars under investigation is illustrated in Figure 4.33. The figure shows that the strength of the OPC mortars improves by all replacement materials after 28 and 56 days curing. The best improvement occurs by an amount of 20% in the OPC/10%SF mix. After 7 days curing only the strength of the SF mix exceeds that of the OPC and at 3 days none of the replacement materials shows significant improvement. It is also observed that at 28 and 56 days the strength values of the OPC/DKut mortars is slight better than those of the OPC/DKt mix, the DKut values exceeds by an average of 2.0 %

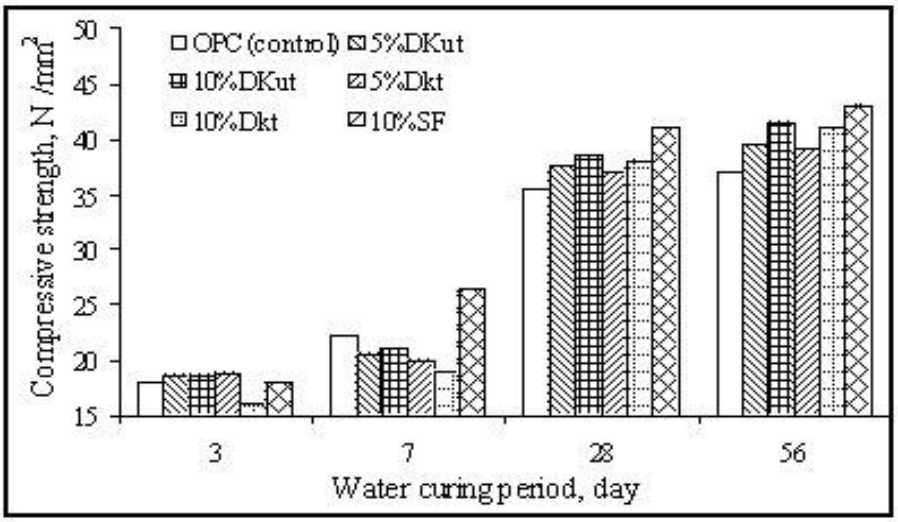

Figure 4.33 Effect of binder type and content on compressive strength of mortar cured with water for various periods.

4.4.2.2 Tensile strength

Figure 4.34 illustrates the effect of replacing the OPC by DK and SF on the tensile strength of mortar specimens cured for 56 days in water. It is clear from the figure that the tensile strength behavior of the mortars under investigation is similar to that of the compressive strength: The tensile strength of the OPC mortar increases steadily with increasing the SF content and that of the OPC/DK mix increases up to 10% replacement ratio then declines. The SF-curve lays higher than those of the OPC/DK mix and the improvement exceeds that of the compressive strength. The individual values of the DKt are slightly better than the strength of the DKut

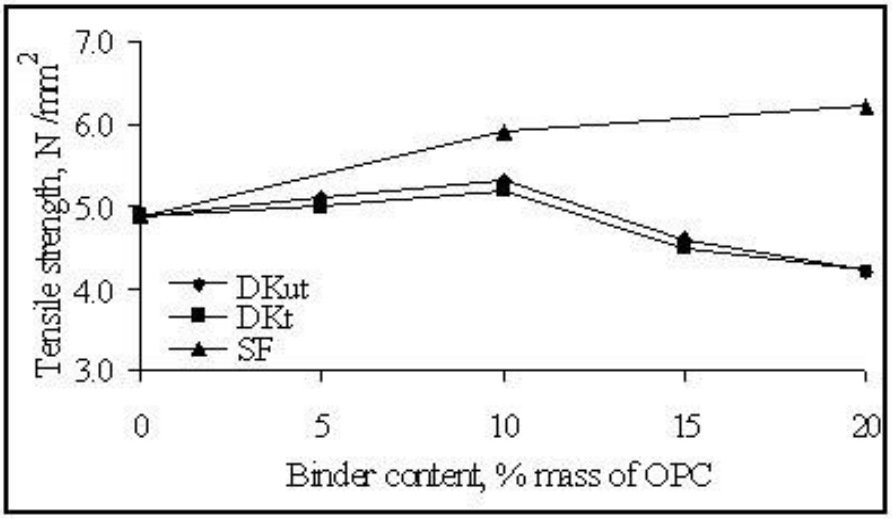

Figure 4.34 Effect of DK content on 56-days mortar tensile strength.

4.4.3 Fluid Transport

The fluid transport properties of the mortars studied were evaluated in terms of the water absorption by capillary action **(**Sorptivity) and water absorption capacity (WA %). The results obtained are discussed below.

4.4.3.1 Water absorption by capillary action (sorptivity)

The relationship between the sorptivity of OPC, OPC/DK and OPC/SF mortars cured in water for 28 and 56 days and the content of the cement replacement material is shown in Figures 4.35a, b, and 4.36.

Figure 4.35a illustrates that the sorptivity of the 28 day-OPC mortar is reduced by up to 10% DK replacement and increases at higher replacement ratio. The DKut leads to slightly lower values than the DKt. In the presence of SF the sorptivity decreases steadily with increasing the SF content. At 10% replacement the DK and SF cause maximum reduction of 9 and 15%, respectively. The same behavior is obtained for the 56-d mortar specimens (Figure 4.35b); the maximum reduction attained in this case for the 10% replacement is 10 and 18% for the DK and SF replacement, respectively. The sorptivity results for the 28 and 56 day-cured mortars with different replacement ratios of the DKut is summarized in Figure 4.35 where, a minimum is seen at a ratio of 10%.

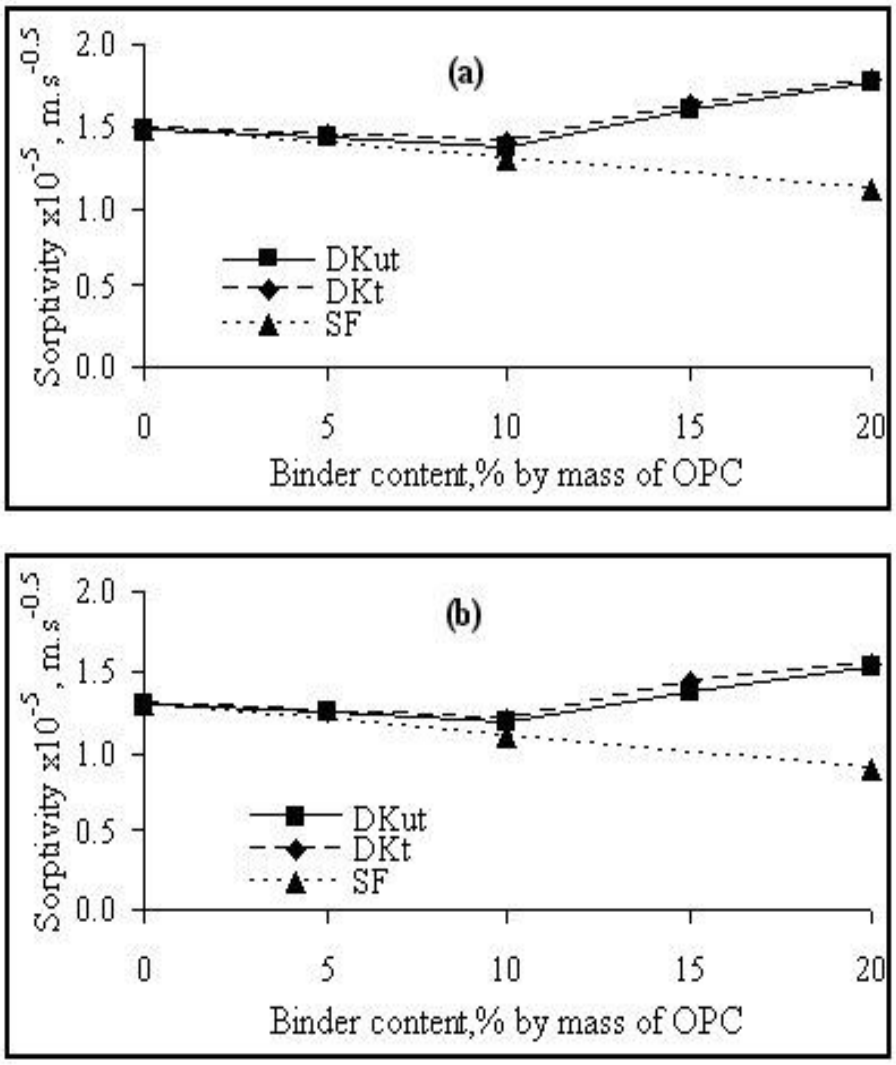

Figure 4.35 Sorptivity of OPC mortar as a function of contents of either DKut or DKt or SF after water curing periods of a) 28 days and b) 56 days.

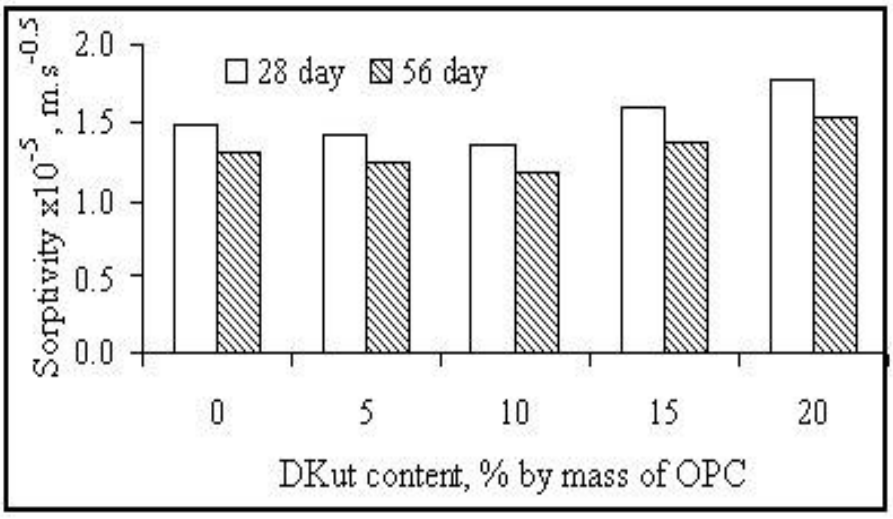

Figure 4.36 Effect of curing period on sorptivity of OPC/DKut mortar.

4.4.3.2 Water absorption by total immersion

The percentages of water absorption (WA %) of the 28 and 56 days-cured mortars under investigation are illustrated in Figures 4.37a, b, and 4.38 as a function of the increasing amount of the cement replacement materials. It is clear from the Figures that the water absorption behavior of the mortars is quite similar to that of the sorptivity: The absorption is reduced by up to 10% DK replacement then increases at higher replacement ratio. The DKut leads to slightly lower values than the DKt. In the presence of SF the absorption decreases steadily with increasing the SF content. In the 28-days cured specimens, 10% replacement with either the DKut or SF causes maximum reduction of ~15%. In the 56-days cured specimens the reduction values by the10% DKut replacement is lower and attains 5% but shows higher values with 10% SF (20% reduction).

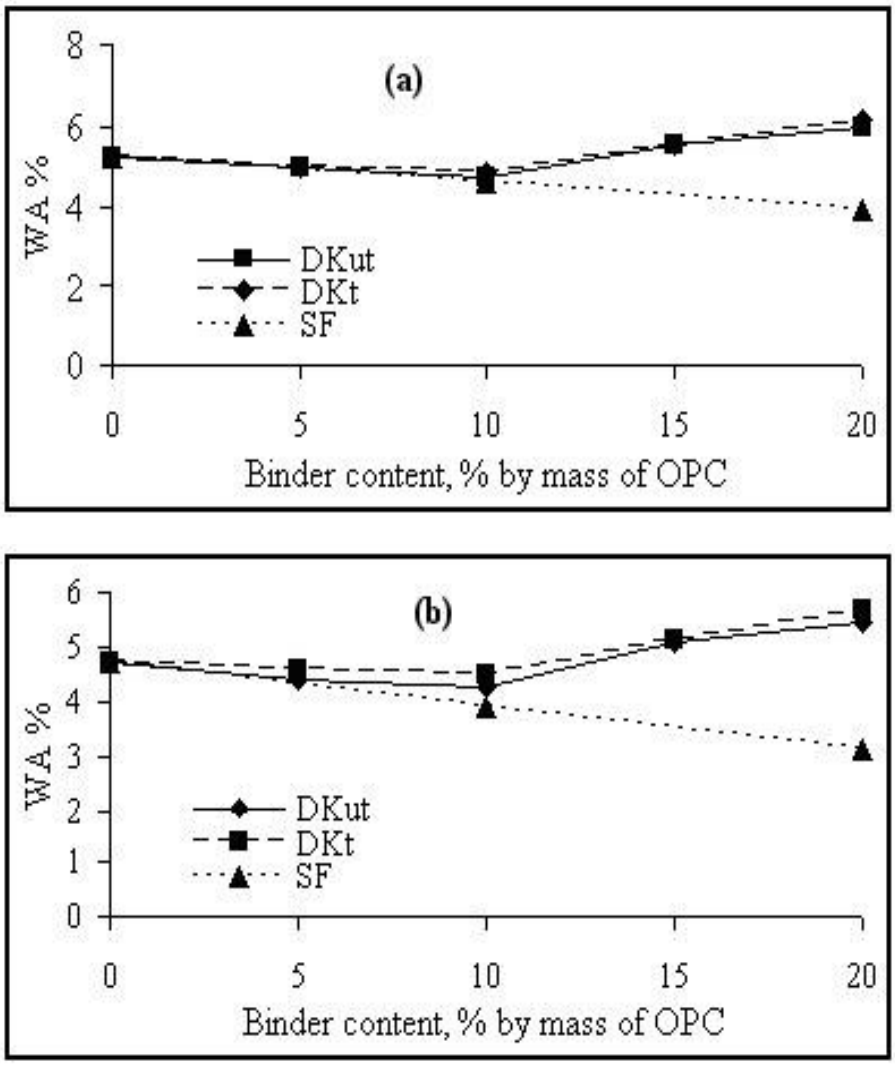

Figure 4.37 Water absorption percent of OPC mortars as a function of contents of either DKut or DKt or SF after water curing periods of a) 28 days and b) 56 days.

The absorption results for the 28 and 56days-cured mortars with different replacement ratios of the DKut is summarized in Figure 4.38 where a minimum is seen at a ratio of 10%.

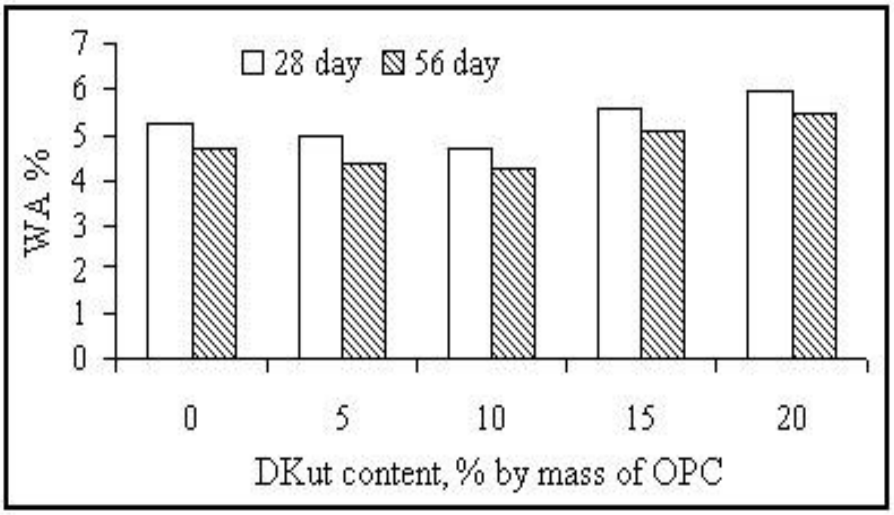

Figure 4.38 Effect of curing period on water absorption of OPC/DKut mortar.

Figure 4.39 shows a relation between the results obtained for the sorptivity and the water absorption capacity which indicate a clear linear correlation for all studied mortars is found and this correlation is valid at different curing age as shown in the Figure. This can provide an explanation to the agreement between the findings obtained from the two considered approaches in this study.

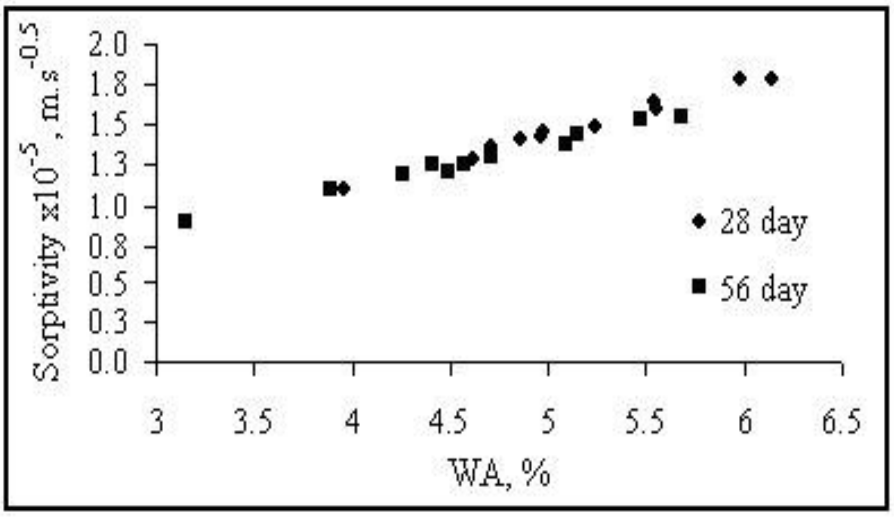

Figure 4.39 Relationship between WA% and sorptivity of OPC mortar incorporating different contents of either DKut or DKt or SF after 28 and 56 days water curing periods.

4.4.4 Durability measurements

The durability aspects of the mortars were assessed by means of measurements for the compressive strength, length and weight changes as well as by the corrosion of the reinforcement. The results obtained are described below.

4.4.4.1 Compressive strength

a- Immersion in water

Figure 4.40 illustrates the compressive strength development for the OPC, OPC/10%DK and OPC/10%SF systems immersed in water for 32 weeks. In general, the compressive strength of the OPC mortars improves in the presence of replacement materials and all values increase with exposure period. The highest values are attained in the SF specimens, followed by the (SF+DKut), DKut then DKt.

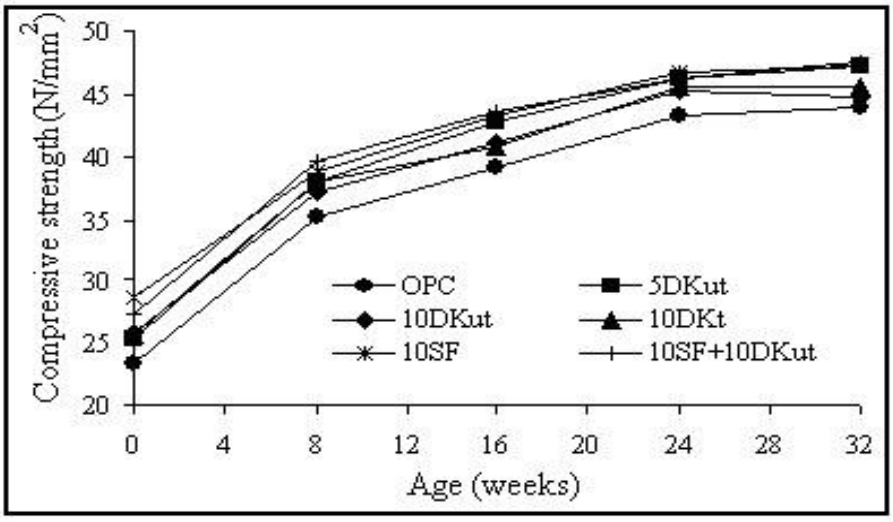

Figure 4.40 Compressive strength for OPC, OPC/DKut, OPC/DKt, OPC/SF and OPC/(SF+DKut) mortar immersed in water.

b- Immersion in sodium sulfate solution

Figure 4.41 illustrates the compressive strength development for the OPC, OPC/10%DK, OPC/10%SF and OPC/(10%DK+10% SF) systems immersed in 5% sodium sulfate solution for 32 weeks. The compressive strength values of the reference OPC mortar increase steadily up to 24 weeks then decrease by an amount of 7% after 32 weeks. The OPC/DK mortars show better values than those of the reference up to 16 weeks but exhibit lower performance at longer exposure period (~8% reduction at 32 weeks). The strength curves of the OPC/SF and OPC/(SF+DKut) are steadily higher than the reference.

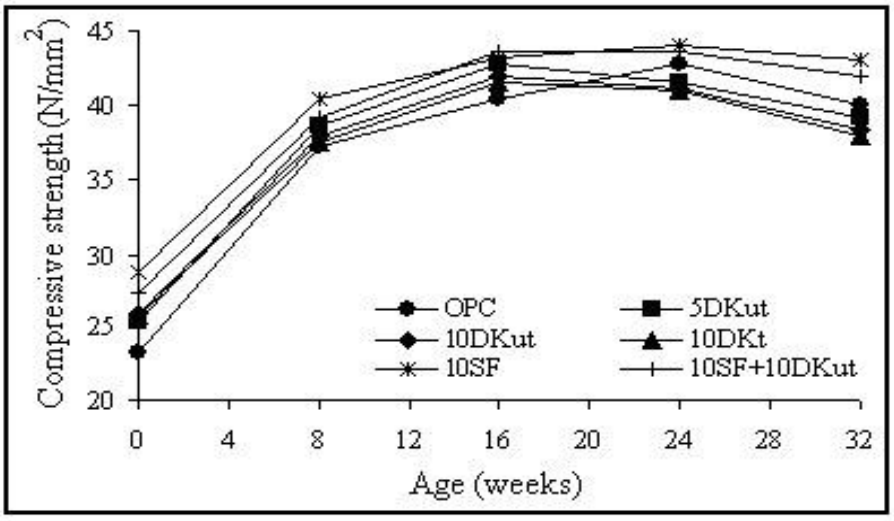

Figure 4.41 Compressive strength for OPC, OPC/DKut, OPC/DKt, OPC/SF and OPC/(SF+DKut) mortar exposed to various wetting exposure regime

The SEM micrograph of OPC and 10%DKut mortar after the strength reduction happened (after 24 weeks) of Figure 4.42 shows ettringite crystals precipitated in the OPC and OPC/10%DK mortar. The double salt appears as fine needle ~10micron in size in the OPC specimen but slightly shorter in the OPC/DK sample.

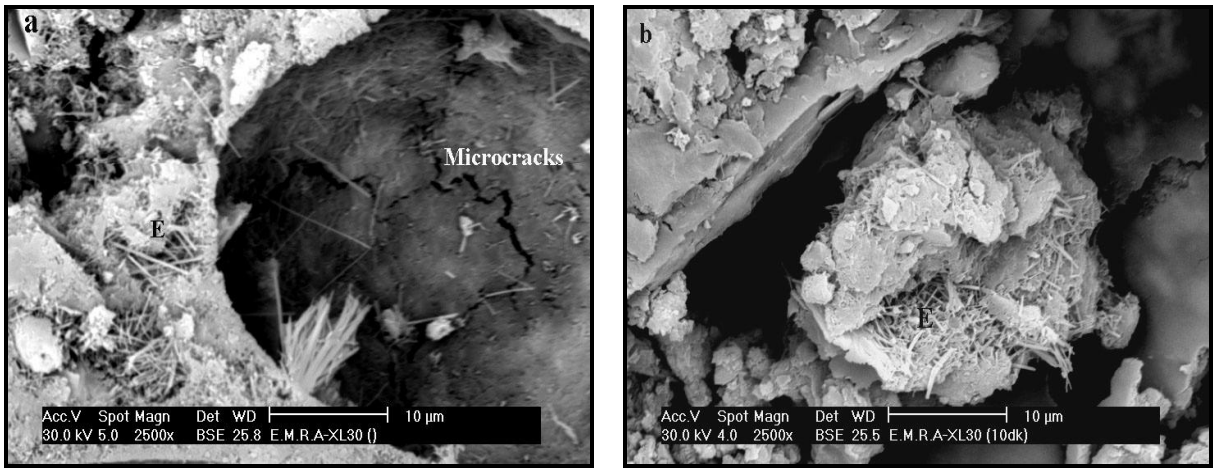

Figure 4.42 SEM micrographs of (a) OPC mix ((b) 10%DKut mix after 24 weeks.

4.4.4.2 Expansion measurements

a- Effect of immersion in water

Figure 4.43 demonstrates the results of the length change of the investigated specimens in water at different exposure time. It is clear from the results that expansion of all mortar

specimens is negligible at the exposure time studied, the values comply with ASTM C1012 (a maximum value of 0.1%).

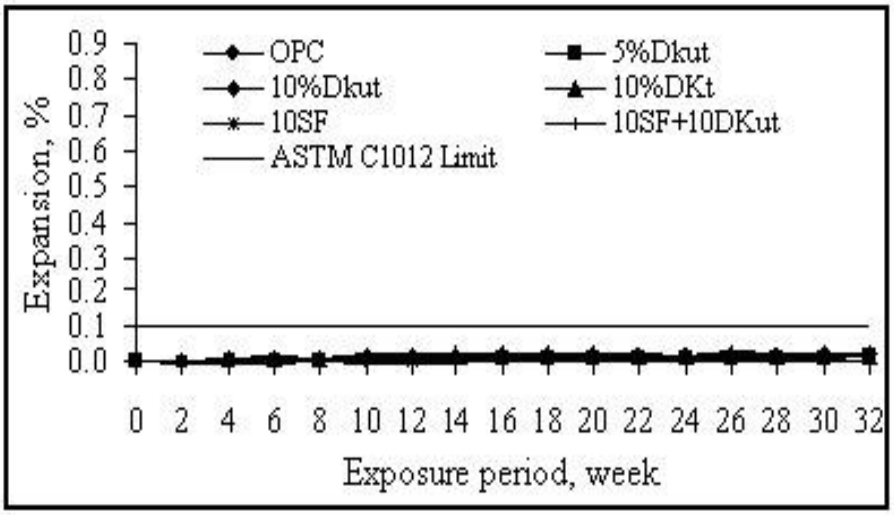

Figure 4.43 % Expansion of OPC, OPC/DKut, OPC/DKt, OPC/SF and OPC/(SF+DKut) mortar immersed in water for 32 weeks.

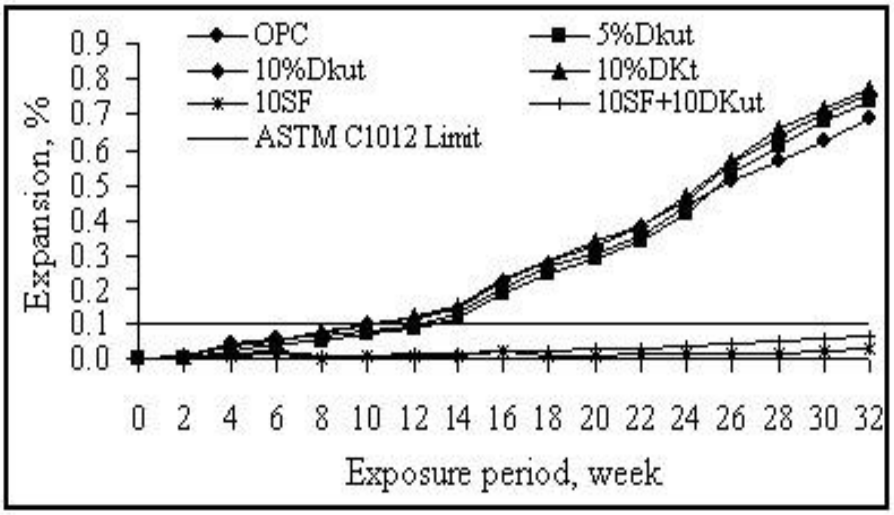

Figure 4.44 % Expansion of OPC, OPC/DKut, OPC/DKt, OPC/SF and OPC/(SF+DKut) mortar immersed in 5%Na_2SO_4 solution for 32 weeks.

b- Effect of immersion in sodium sulfate solution

In 5% sodium sulfate solution the expansion of the mortars prepared with OPC/10%SF and OPC/10%SF+10%DKut was lower than the standard limit of 0.1% over the studied period. Mortars made of OPC, OPC/DK exceeded, however, the standard value after 10 to 14 weeks and attained values of ~0.8% after 32 weeks; the greater the amount of DK in the sample the earlier the expansion and the higher the expansion values at 32 weeks. After 24 weeks the OPC/DK curves lay higher than the reference OPC specimen as shown in Figure 4.44. After

32 weeks exposure, the OPC and OPC/DK mortars with ~ 0.8% expansion deteriorated and several edge hair cracks were observed as shown in Figure 4.45.

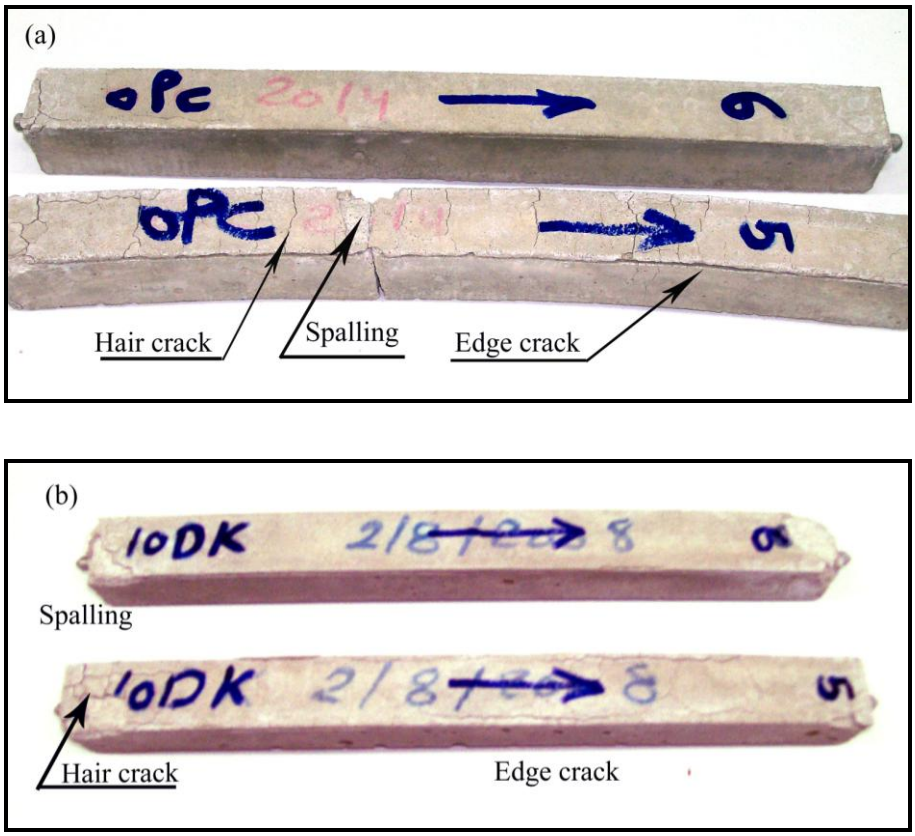

Figure 4.45 Length change specimens subjected to wetting exposure regimes of 5%Na_2SO_4 solution (at the end of exposure period) a) OPC mortar and b) OPC/10% DKut mortar.

c- Effect of wet/dry cycles

The expansion behavior of the mortar specimens immersed in water as well as in sodium sulfate solution then left to dry is illustrated in Figures 4.46 (a, b). The figures show that no expansion occurs in all samples subjected to wet/dry cycles in water, the specimen shrink, however, with maximum value of ~0.04% over the period studied. On the other hand significant expansion values are observed increasingly in the OPC and OPC/DK samples subjected to wet/dry cycles in sodium sulfate solution starting from 18 weeks until the 32 weeks, the maximum expansion value attained is ~0.4% which obviously lower that that monitored in the steadily wet samples. The expansion of the OPC/5%DK mortar specimens exceeded the specification value at 22 weeks showing a slower expansion process. After 32 weeks the expansion of OPC/DK samples is found to exceed that of the OPC systems by a maximum amount of 12%. After 32 weeks exposure, the OPC and OPC/DK mortars with ~ 0.4% expansion deteriorated and several edge hair cracks were observed.

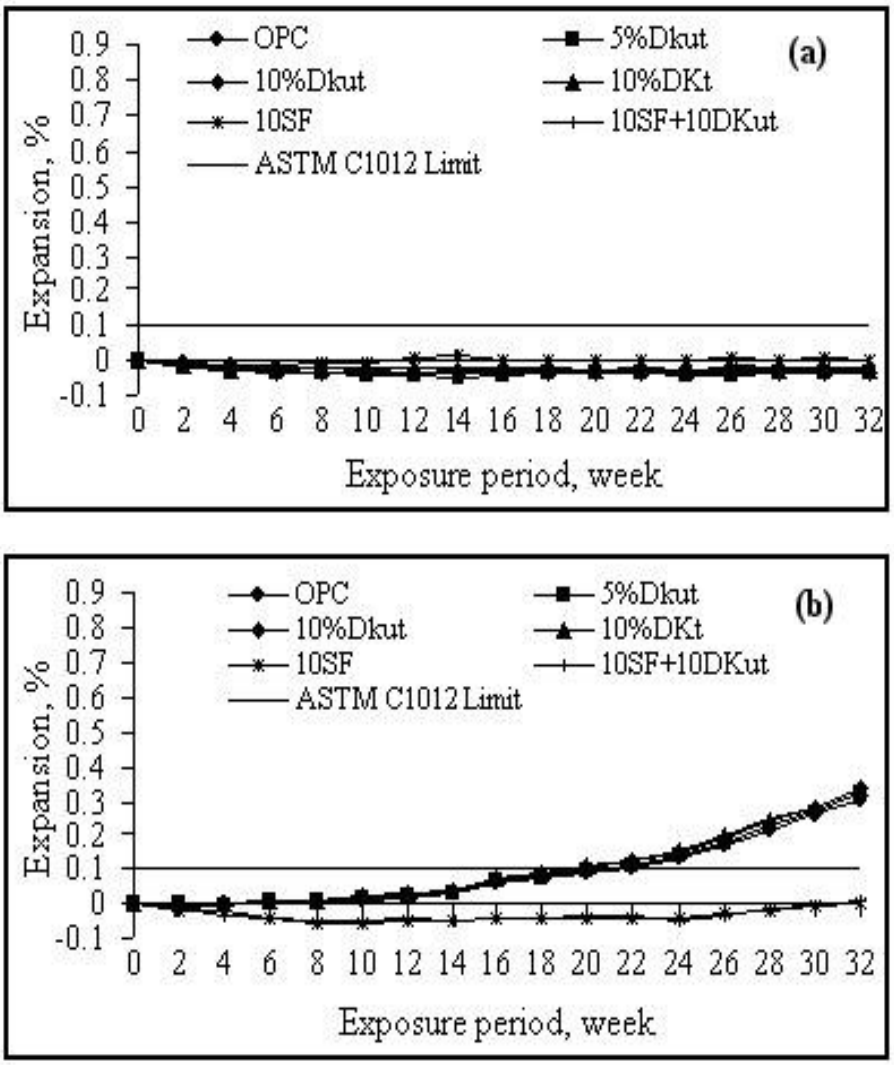

Figure 4.46 % Expansion of OPC, OPC/DKut, OPC/DKt, OPC/SF and OPC/(SF+DKut) mortar exposed to wetting/drying exposure regime in a) water and b) 5%Na_2SO_4 solution.

d- The expansion behavior after the drying period

At the end of drying period, the expansions of the specimens was measured; the samples were steadily immersed in water and in 5% Na_2SO_4 solutions; the results obtained are shown in Figures 4.47a and b. Similar trends were found for the tested specimens at the end of drying period as those found at the end of wetting period. However, the values of % expansion measured for such specimens at the end of drying period are lower than that measured at the end of wetting period.

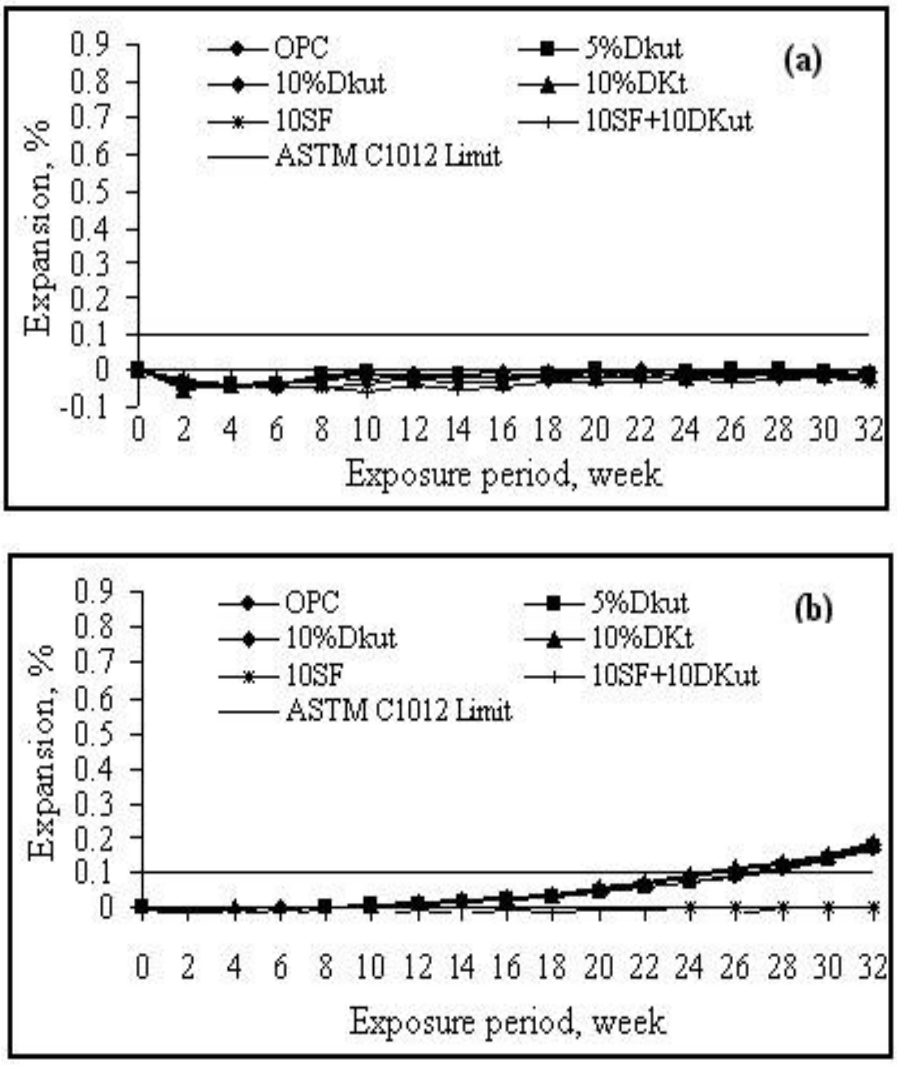

Figure 4.47 % Expansion of OPC, OPC/DKut, OPC/DKt, OPC/SF and OPC/(SF+DKut) mortar exposed to wetting/drying exposure regime in a) water and b) 5%Na_2SO_4 solution (at the end of drying period).

4.4.4.3 Weight change measurements

a- Effect of immersion

Figure 4.48a illustrates the results of the weight change of the investigated specimens in water at different exposure time. It is clear from the results that the % weight gain of all mortar specimens is negligible at the exposure time studied. In 5% sodium sulfate solution the weight of the OPC, OPC/DK and OPC/SF increase steadily with exposure time; the weight gain curves of the OPC/10%SF and OPC/10%SF+10%DK lay significantly lower than those of the remaining systems as shown in Figure 4.48b.

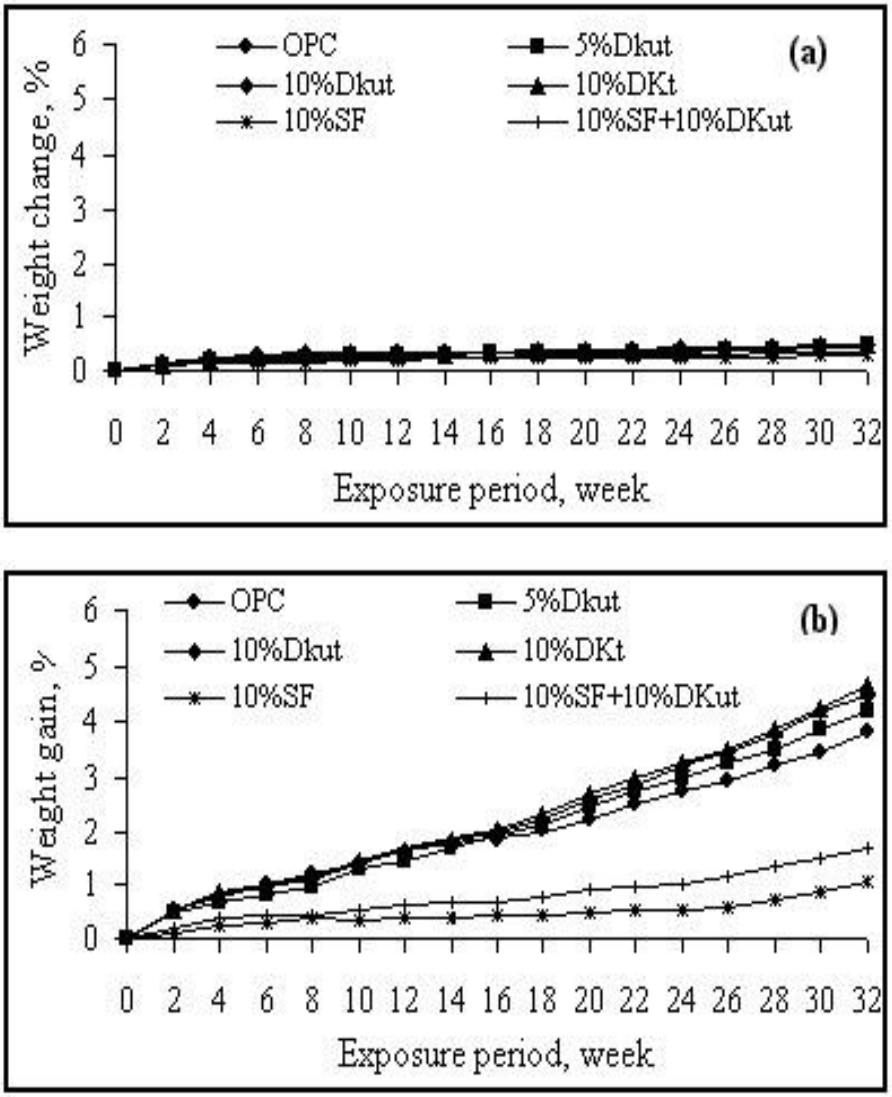

Figure 4.48 % Weight gain of OPC, OPC/DKut, OPC/DKt, OPC/SF and OPC/(SF+DKut) mortar immersed in a) water and b) 5%Na_2SO_4 solution for 32 weeks.

b- Effect of wet/dry cycles

The weight change of the mortar specimens immersed in water as well as in sodium sulfate solution then left to dry is illustrated in Figures 4.49 (a, b). Figures show clear steady loss in the weight of the mortars made of OPC/10SF and OPC/10%SF+10%DK when the wet/dry cycles are carried out in water; in sodium sulfate solution, however, the extent of loss is reduced at long exposure time. The mortars prepared of OPC and OPC/DK exhibit a weight loss at longer age of the wetting/drying cycles in water but increase steadily in weight when the cycles are performed in sodium sulfate solution.

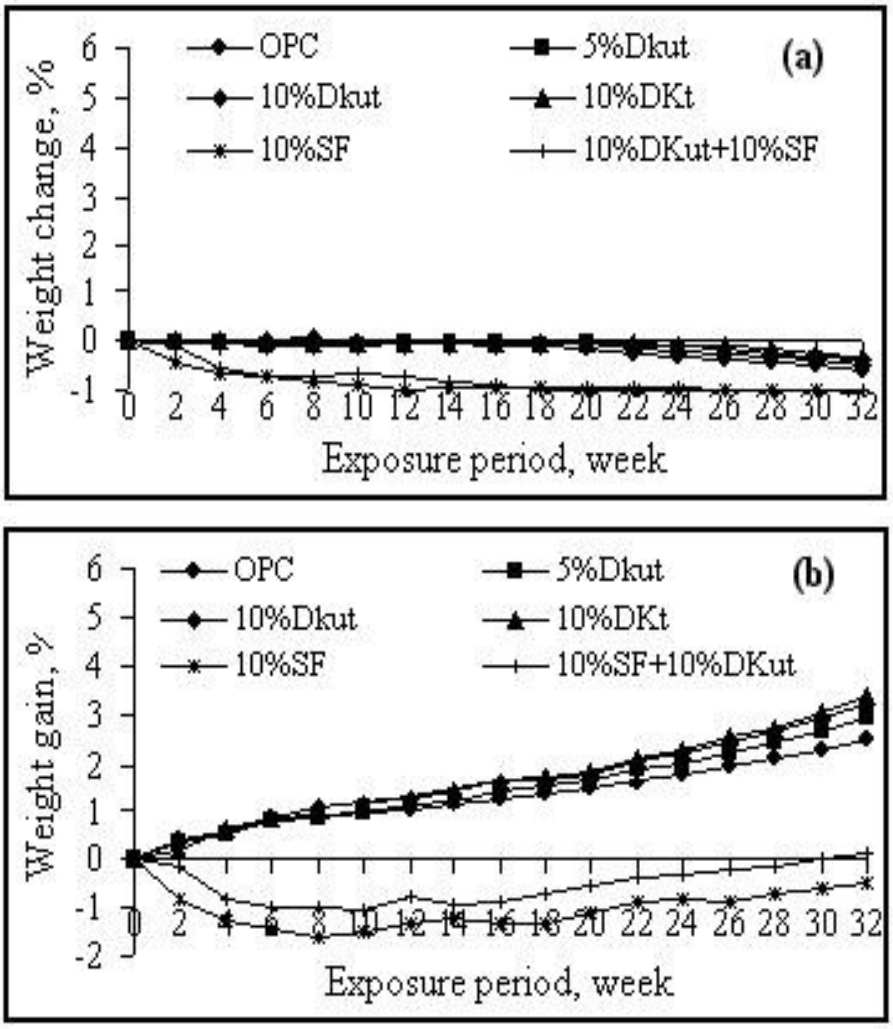

Figure 4.49 % Weight gain of OPC, OPC/DKut, OPC/DKt, OPC/SF and OPC/(SF+DKut) mortar exposed to wetting/drying exposure regime in a) water and b) 5%Na_2SO_4 solution .

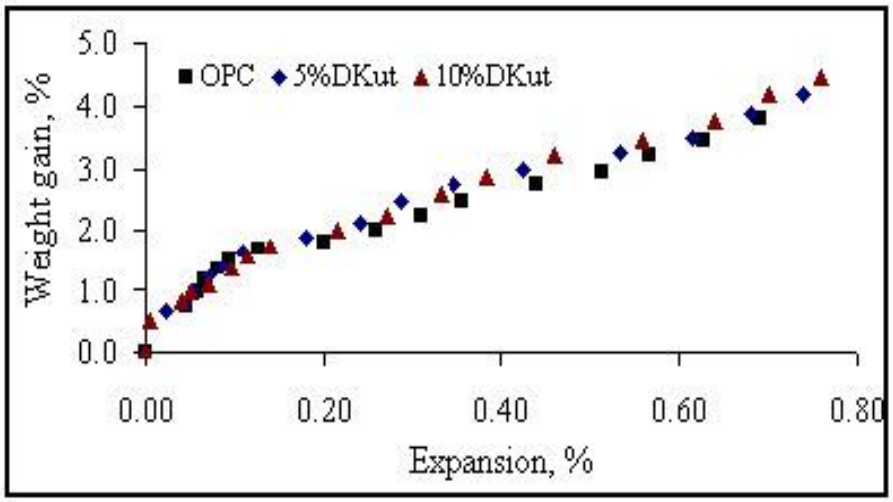

Figure 4.50 Relationship between % expansion and weight gain of OPC mortar containing different contents of DKut.

4.4.4.4 Correlation between the expansion and weight change

Figure 4.50 shows the correlation between the results obtained from the measurement of the expansion and the weight change of the mortars and indicates a direct relation with a satisfactory straight line.

4.4.4.5 Corrosion measurement

The corrosion activity of reinforced mortar specimens prepared of OPC as well as of OPC with replacement materials are expressed in terms of the half-cell potential according to ASTM C876-80. Simultaneous to the half-cell potential tests, the corrosion current density measurements are monitoring using zero resistance ammeter. The results obtained are described below.

4.4.4.5.1 The corrosion potential

a- Immersion in water

Figure 4.51 illustrates the change in the half-cell potential measurements of the reinforced mortar made of OPC, OPC with the different replacement materials, as a function of exposure time. It is clear from the figure that the corrosion potential of the mortar increase slightly with increasing the exposure period, the results of all specimens are close to each other, their average values indicate that there is no probability for the corrosion to occur compared to the limits of the ASTM C876, which states the absence of corrosion of steel at potentials values less negative than -200 mV, CSE.

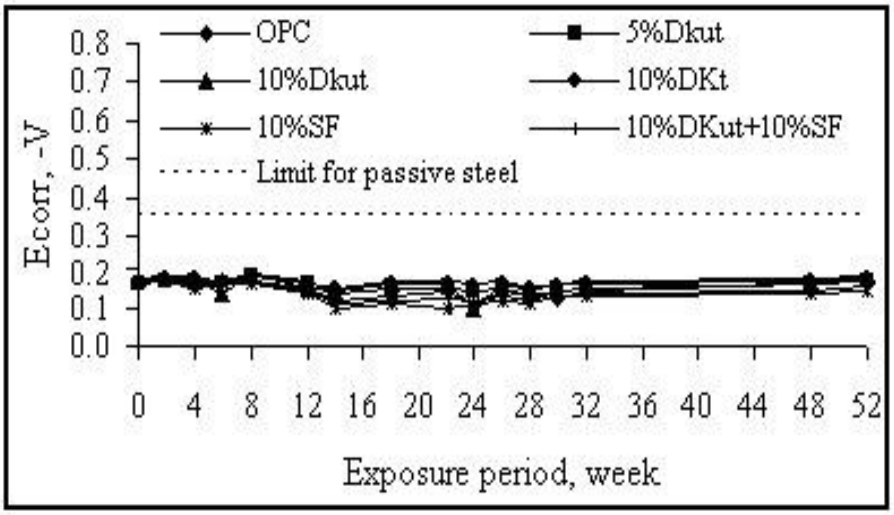

Figure 4.51 Corrosion potentials for OPC, OPC/DKut, OPC/DKt, OPC/SF and OPC/(SF+DKut) mortar immersed in water.

b- Immersion in sodium chloride solution

Figure 4.52 illustrates the corrosion potential values for the mortar specimens immersed in 5% NaCl solution at exposure time up to 52 weeks. The results show that the potential values increase with increasing the exposure period for all specimens and that according to ASTM C876 (the steel potentials are more negative than -350 mV, CSE).a great possibility exists for the corrosion of the reinforcement to take place. The highest potential is found for the OPC/DKt specimen and the least for OPC/SF followed by OPC/SF+DK specimen.

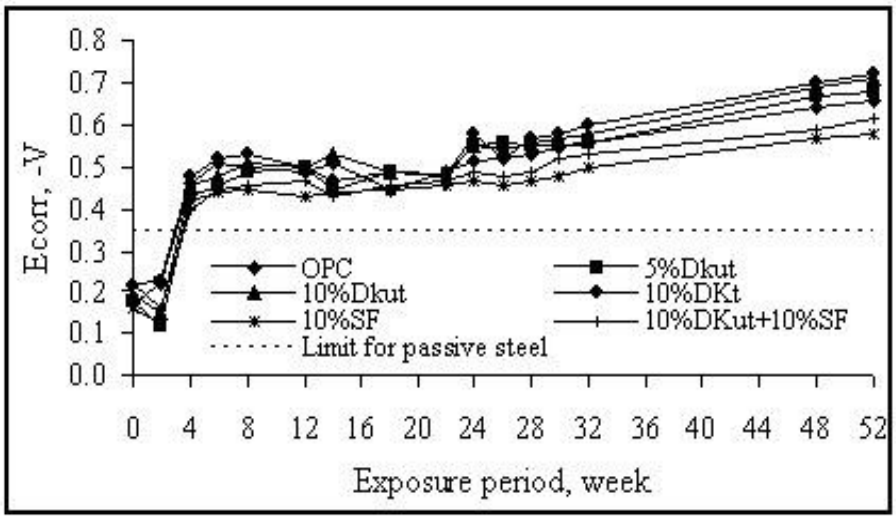

Figure 4.52 Corrosion potentials for OPC, OPC/DKut, OPC/DKt, OPC/SF and OPC/(SF+DKut) mortar immersed in 5% NaCl solution.

c- Effect of the wet/dry cycle

The results obtained on the effect of the wet/dry cycle on the corrosion potential of the mortar specimens in water and in 5% NaCl solutions are shown in Figures 4.53 a, b. All mortars have quite similar behavior in the case of water (Figure 4.53a) but increase significantly after 4 weeks in NaCl solution (Figure 4.53b). The best performance in the chloride solution is due to the OPC/SF and OPC/SF+DK samples.

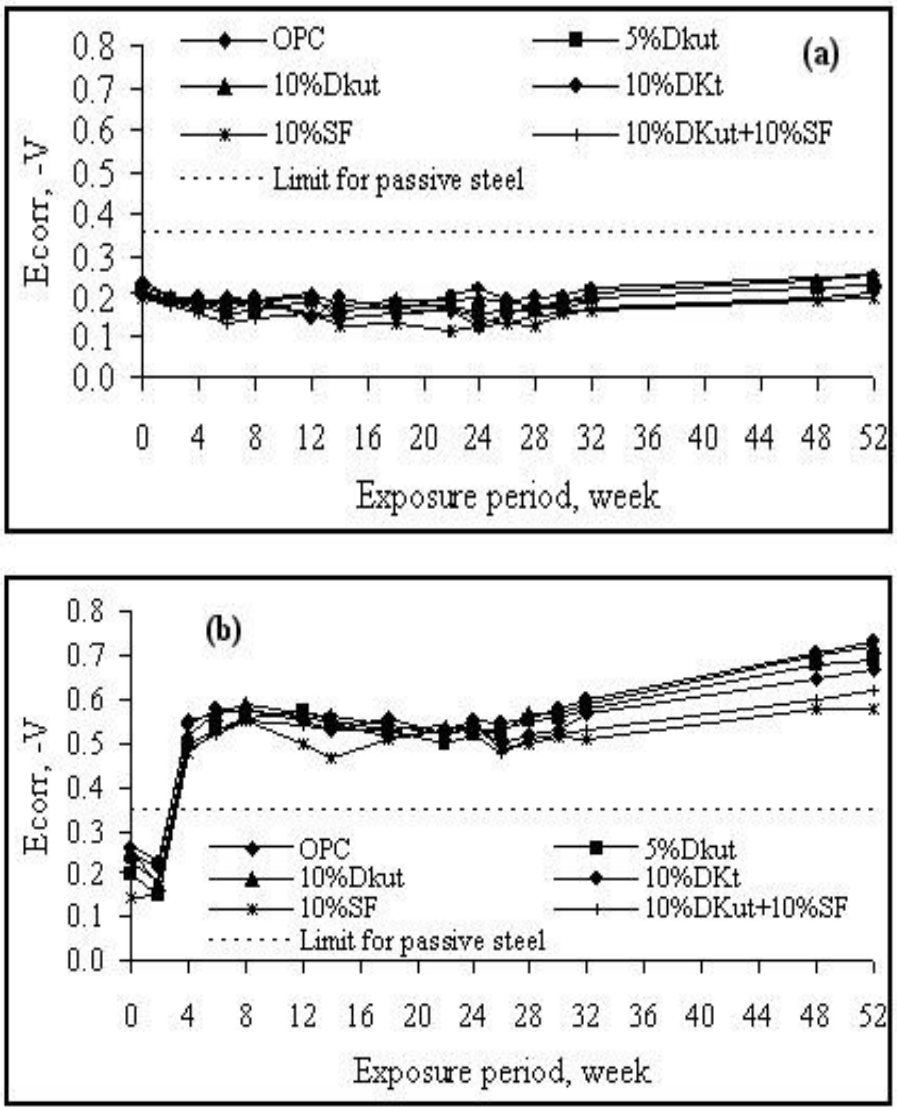

Figure 4.53 Corrosion potentials for OPC, OPC/DKut, OPC/DKt, OPC/SF and OPC/(SF+DKut) mortar exposed to wetting/drying exposure regime in a) water and b) 5%NaCl solution.

4.4.4.5.2 Current density

a- Immersion in water

Figure 4.54 illustrates the change in the corrosion current density (corrosion rate) of the reinforced mortar made of OPC, OPC with the different replacement materials, as a function of exposure time. It is clear from the figure that the values of the increase in the corrosion rate is insignificant for all specimens, According to Andrade et al, (1988), the corrosion of reinforcing steel does not occur if the corrosion rate value is less than 0.1 $\mu A/cm^2$

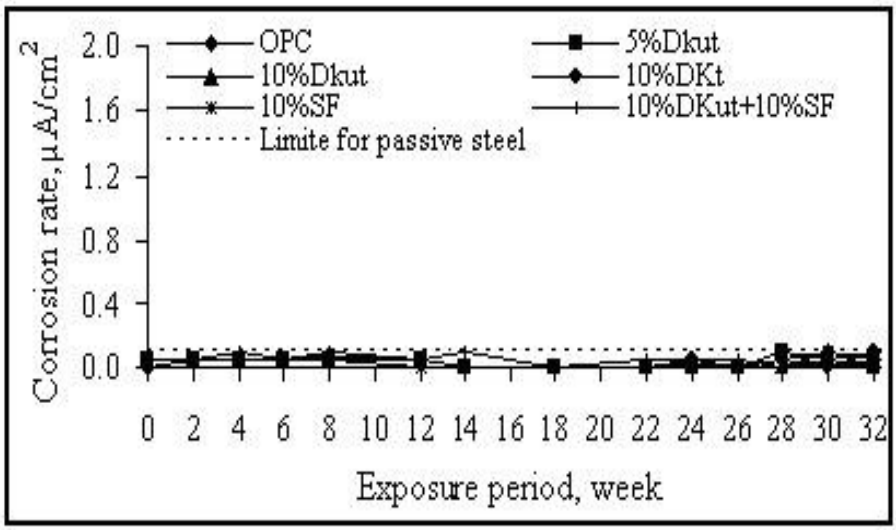

Figure 4.54 Corrosion rate for OPC, OPC/DKut, OPC/DKt, OPC/SF and OPC/(SF+DKut) mortar immersed in water.

b- Immersion in sodium chloride solution

Figure 4.55 illustrates the corrosion rate values for the mortar specimens immersed in 5% NaCl solution at exposure time up to 52 weeks. The results show that the corrosion rate values increases with exposure period for all the tested specimens. The OPC/DKut specimens show a slightly better initial corrosion resistance than OPC otherwise all specimens indicate greater corrosion probability than OPC. The best performance is again observed in the SF-bearing mortar specimens.

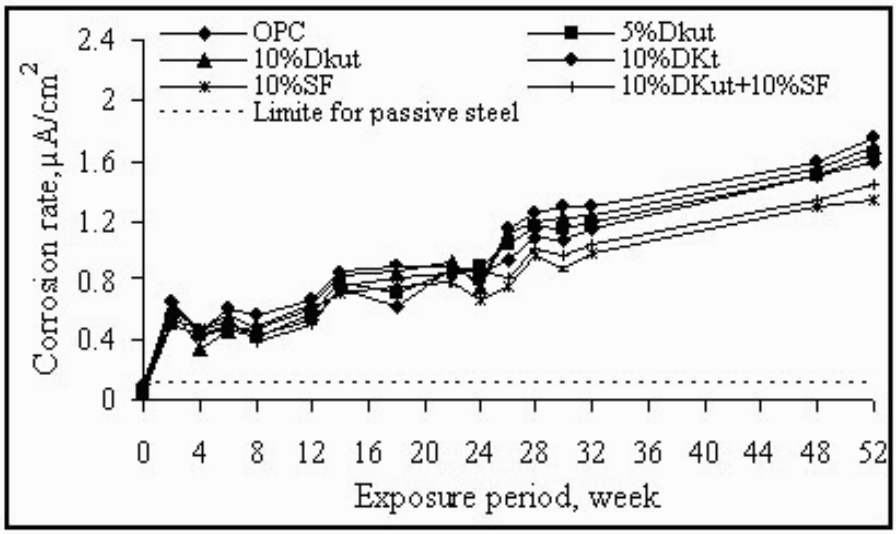

Figure 4.55 Corrosion rate for OPC, OPC/DKut, OPC/DKt, OPC/SF and OPC/(SF+DKut) mortar immersed NaCl solution.

c- Effect of wet-dry cycle

The results obtained on the effect of the wet/dry cycle on the corrosion potential of the mortar specimens in water and in 5% NaCl solutions are shown in Figure 4.56. All mortars have low corrosion probability and quite similar behavior in the case of water (Figure 4.56a) but increase significantly after 4 weeks in NaCl solution (Figure 4.56b). The best performance in the chloride solution is due to the OPC/SF and OPC/SF+DK samples. The behavior is similar to the sulfate exposure

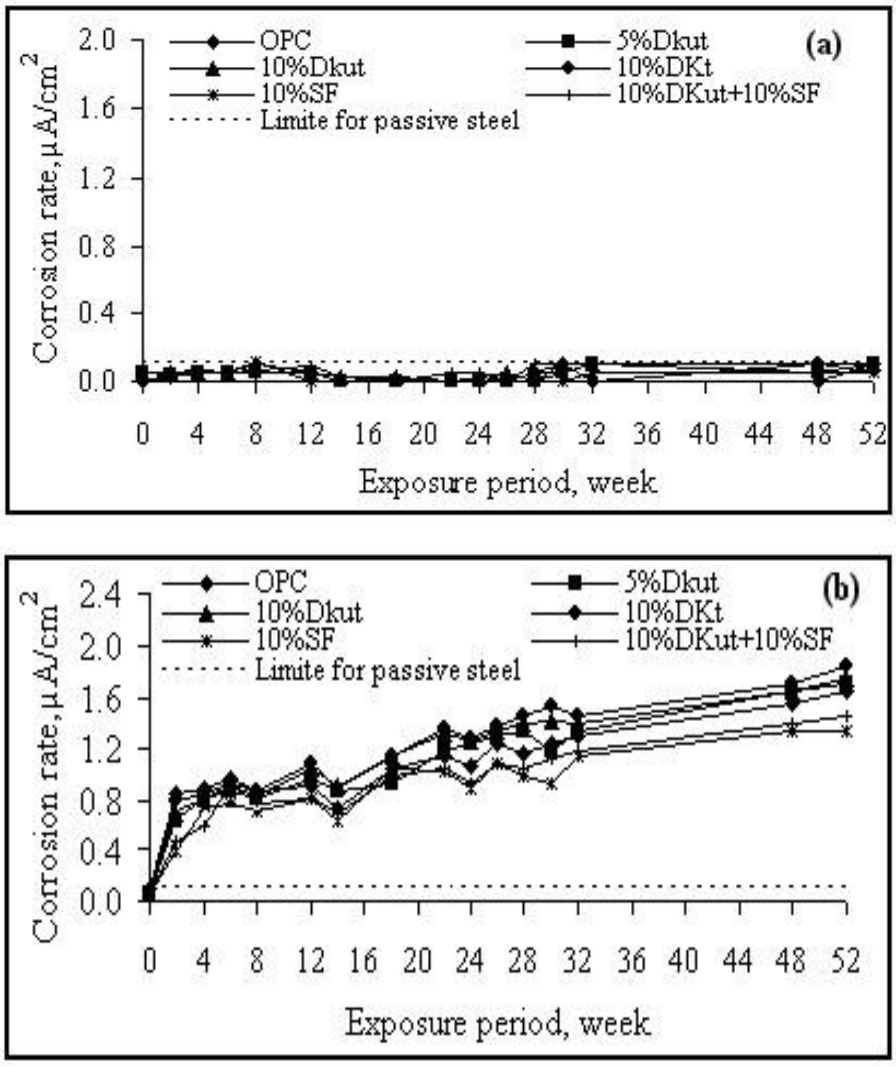

Figure 4.56 Corrosion rate for OPC, OPC/DKut, OPC/DKt, OPC/SF and OPC/(SF+DKut) mortar exposed to wetting/drying exposure regime in a) water and b) 5%NaCl solution.

4.4.4.5.3 Correlation diagrams

Figure 4.57 shows the correlation between the results obtained from the measurement of the corrosion potential and corrosion rate of the mortars and studied OPC and DKut mortars. This

provides an explanation to the agreement between the findings obtained from the two considered approaches in this study.

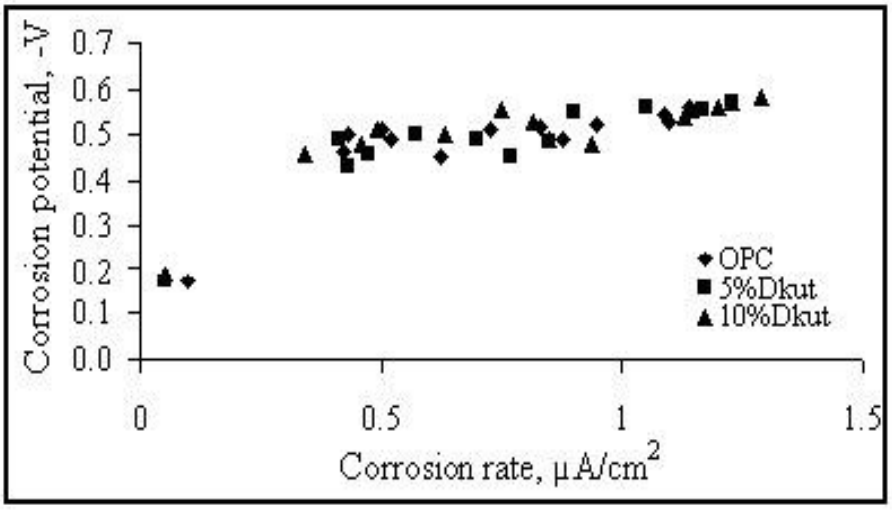

Figure 4.57 Relationship between corrosion potential and corrosion rate of reinforcing steel embedded in OPC or OPC/DKut mortar.

Another correlation between the rate of degradation of both hardened cement paste and reinforcement is shown in Figure 4.58; the percentage expansion is plotted versus the corrosion potential measurements. The figure shows a significant increase in the corrosion activity of reinforcement with increasing expansion from 0 to 0.1%, followed by a fairly steady-state increase of corrosion with increasing the %expansion. This means that the degradation process of both HCP and reinforcing steel are strongly related and dependent.

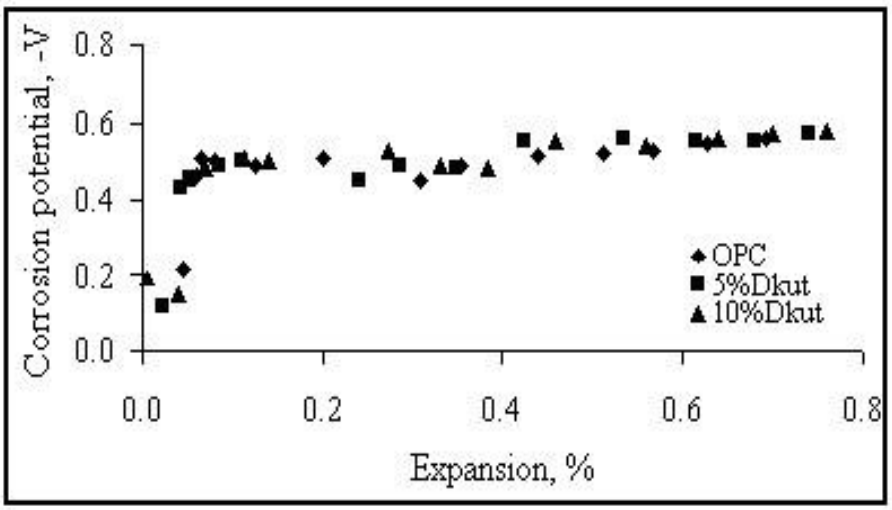

Figure 4.58 Relationship between % expansion and corrosion activity of reinforcement of OPC or OPC/DKut mortar

4.5 Concrete

4.5.1 Fresh Properties

To examine the fresh properties of OPC concrete mixes containing either DKut or DKt contents of 0, 5 and 10%, or 10%SF as cement replacement material, both slump and weight per unite volume of fresh OPC concrete were measured directly just before casting the molds in this study as an indicative measure for the workability of concrete.

The effect of DKut, DKt and SF on the workability and unit weight of OPC concrete are presented in Table 4.6. It is clear that the incorporation of either DKut or DKt led to a reduction in the concrete slump, this effect increases with increasing their content. The reduction is more significant in OPC/DKt mix than that contain DKut. The amount of reduction reaches about 26, 37 and 42% for 10% replacement of the OPC by DKut or DKt or SF, respectively. These results confirm those of mortar flowability.

Table 4.6 Slump and unit weight of OPC concrete containing either DK two forms or SF as a cement replacement materials.

Mix No.	Mix code	Slump, mm	Unit weight, kg/m^3
1	OPC	95	2415
2	95%OPC/5%DKut	85	2385
3	90%OPC/10%DKut	70	2365
4	95%OPC/5%DKt	75	2390
5	90%OPC/10%DKt	60	2370
6	90%OPC/10%SF	55	2375

It is very important to mention that the incorporation of either DK two forms or SF to OPC concrete causes a notable reduction in their unit weight (see Table 4.6). This effect is more pronounced with DKut than DKt and increases with increasing their content. These results would be helpful when the concept of designing of reinforced concrete elements is considered. Where, the reduction in unit weight of concrete will result in reducing the dead loads of the various structural elements causing a notable reduction in the concrete dimensions.

4.5.2 Hardened properties

4.5.2.1 Compressive strength

The results shown in Figure 4.59 confirm that replacement OPC by either DKut or DKt increase the concrete compressive strength with increasing DK content and curing period. The individual values of the DKut are slightly better than the strength of the DKt. The best improvement occurs by replacing OPC by 10%DKut. The amount of improvement reaches 10% higher than OPC mix. Replacing OPC by 10%SF results higher compressive strength than those of the OPC/DK mix and amount of improvement reaches 15% higher than OPC mix after 90 days curing period. This result confirm the previous mortar results

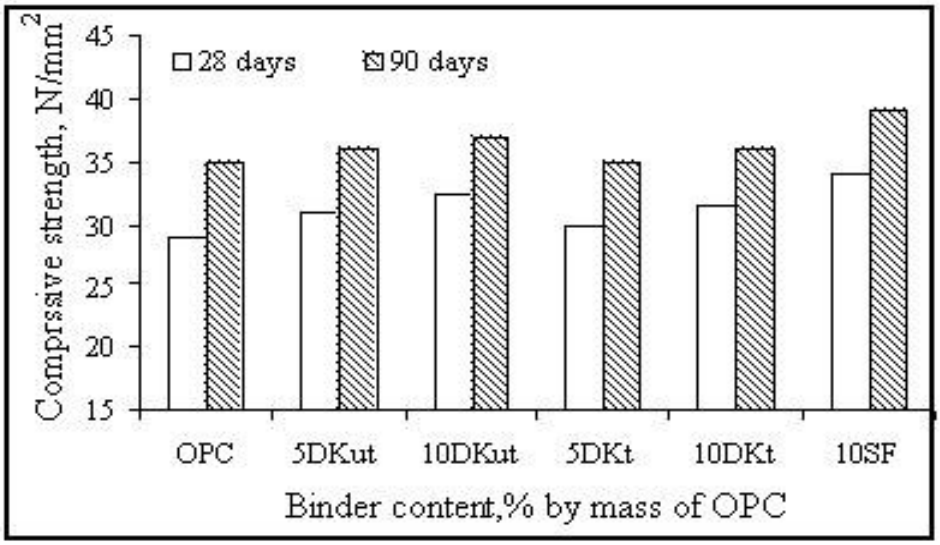

Figure 4.59 Effect of binder type and content on 28 and 90 days OPC concrete compressive strength.

4.5.2.2 Splitting tensile strength

The results illustrated in Figure 4.60 emphasize that, replacement OPC by either DKut or DKt increase the splitting tensile strength of OPC concrete. Similar to the previous compressive strength results, the amount of improvement was increased by increasing DK content and the curing age. Similar results were obtained for OPC concrete containing SF. The maximum increase was obtained by replacing OPC by 10%SF followed by 10%DKut mix. The amount of increase reaches about 9 and 6% for SF and DKut mixes, respectively, after curing period of 90 days.

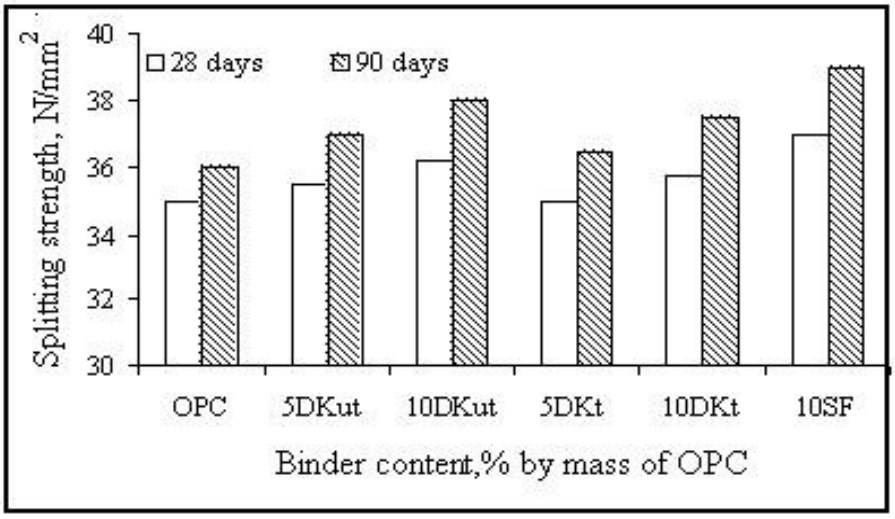

Figure 4.60 Effect of binder type and content on 28 and 90 days OPC concrete splitting tensile strength.

4.5.2.3 Flexural strength

The flexure strength can be expressed in terms of modulus of rapture, which is the maximum stress at rupture. The results of this investigation are illustrated in Figure 4.61. The results shown in the Figure emphasize that the behavior of all studied concrete under flexure is similar to both compressive and splitting tensile strength. The best improvement occurs by replacing OPC by 10% SF followed by 10%DKut. The amount of improvement in the concrete modulus of rupture reaches about 20 and 10% for SF and DKut mixes, respectively, after curing period of 90 days.

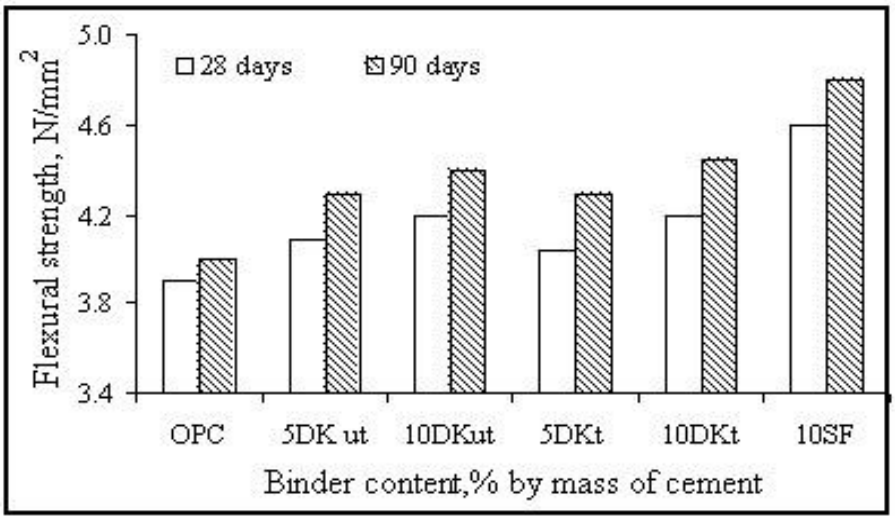

Figure 4.61 Effect of binder type and content on 28 and 90 days OPC concrete modulus of rupture.

The results of 4-point bending test of OPC concrete mix containing (0, 10 and 20%DKt by mass of OPC) after 28 days are shown in Figures 4.62 to 4.64. The results shown in Figure 4.62 illustrate the effect of DKt incorporation on vertical displacement at mid span (deflection) for notched concrete beams. The Figure emphasizes that the inclusion of 10%DKt in OPC concrete mixes increases the peak load at which failure occur while, decreases vertical displacement at mid span at any applied load until reaching the peak load. On the other hand, the inclusion of 20%DKt has opposite effect. This means that 10%DKt inclusion improves the concrete modulus of rapture, while 20%DKt inclusion oppositely effect. The maximum amount of increase in the peak load reaches 5% and the corresponding amount of reduction in the vertical displacement reaches 30% as a result of 10%DKt inclusion.

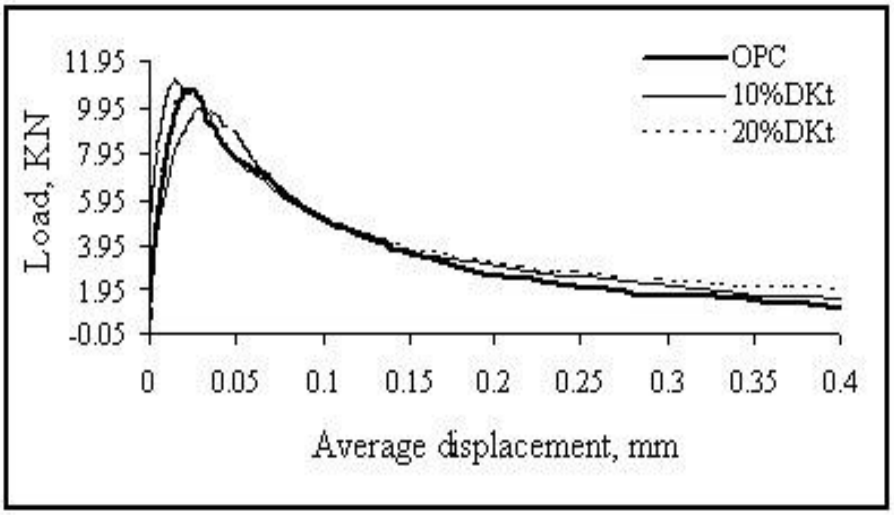

Figure 4.62 Load-displacement curve of OPC concrete containing different content of DK.

The results shown in Figure 4.63 illustrate the effect of DKt incorporation on crack mouth opening displacement (CMOD) for OPC concrete beam notched at mid span subjected to 4-poit bending test. The Figure emphasizes that the inclusion of 10%DKt in OPC concrete mixes decreases the CMOD at any load value up to the peak load and also, increases the load value at which the first crack start to propagate. On the other hand, the inclusion of 20%DKt has opposite effect. The maximum amount of reduction in CMOD value reaches 15%, while, the amount of the increase in the value of crack initiation load reaches 40% as a result of10%DKt inclusion. This means that, 10%DKt inclusion resist the crack propagation at any applied load value up to the peak.

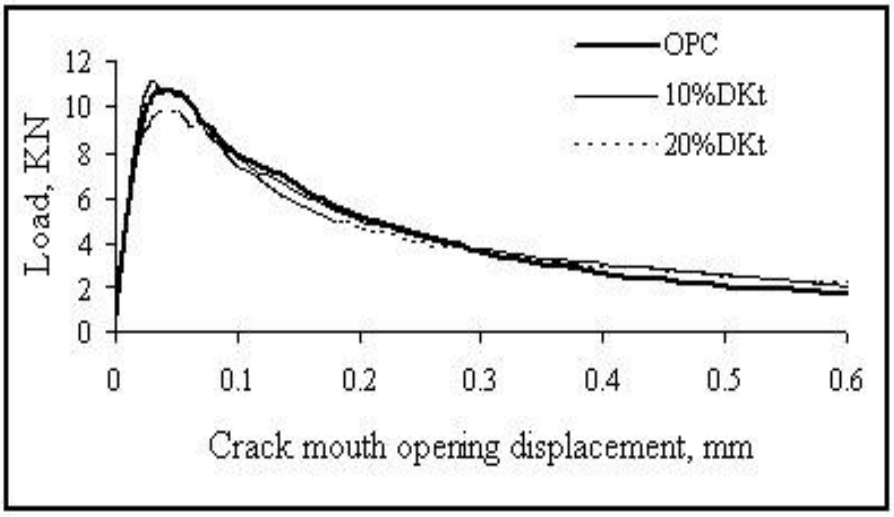

Figure 4.63 Load-crack mouth opening displacement curve of OPC concrete containing different content of DK.

The effect of DKt incorporation on CTOD value for concrete beam notched at mid span and subjected to 4-poit bending test is shown in Figure 4.64. The figure illustrates that CTOD results is similar to that of CMOD; i.e. the inclusion of 10%DKt in OPC concrete mixes decreases the CTOD at any load value up to the peak load. The maximum amount of reduction value reaches 70% higher than OPC concrete mix.

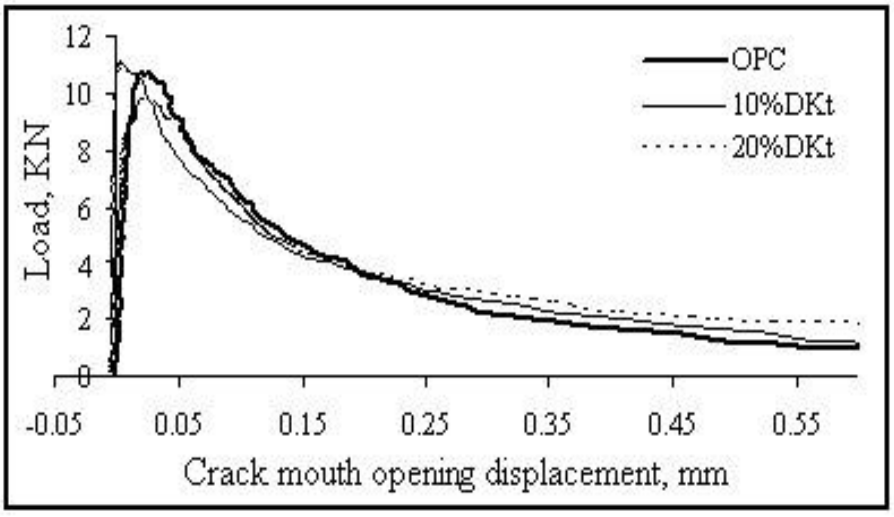

Figure 4.64 Load-crack tip opening displacement curve of OPC concrete containing different content of DK.

4.5.3.4 Stress-Strain behavior

Figure 4.65 shows the relationship between the applied stress and the resulting longitudinal strain for OPC, 10%DKt and 20%DKt concretes at curing age of 28 days. Stress-strain curves for 10%DKt concrete was found to be comparable with that of the OPC concrete. The

ascending (pre-peak) part of the stress-strain curve of both OPC and 10%DKt concrete is parallel to each other. This means that the elastic moduli (slop of the ascending part) of both concrete are quit similar. However, the concrete containing 10%DKt curve starts to deviate from linearity to the horizontal prior to the peak load at higher stress/strength ratio than that of OPC concrete. According to Slate et al 1986, deviation of stress-strain curve from linearity is related to propagation of the microcracks in concrete. Most of these cracks occur at the cement paste-aggregate interface. This is due to the relative weakness of this interface along with the concentration of stresses resulting from the elastic mismatch between the cement paste and the aggregate. This means that unstable microcracks start to propagate in 10%DKt concrete at higher stress/strength ratio than that of OPC concrete. The values of stress/strength ratio were found to be 90, 95 and 87% for OPC, 10%DKt and 20%DKt concrete. respectively. The descending (post-peak) part of the stress-strain curve of both concrete which represents the strain softening seems to be different. The descending part of the stress-strain curve of 10%DKt concrete is less steeper than that of OPC concrete. Also, according to Slate et al 1986, the less steeper the descending part of the stress-strain curve the more ductile the behavior. This means that 10%DKt concrete is less brittle than that of OPC.

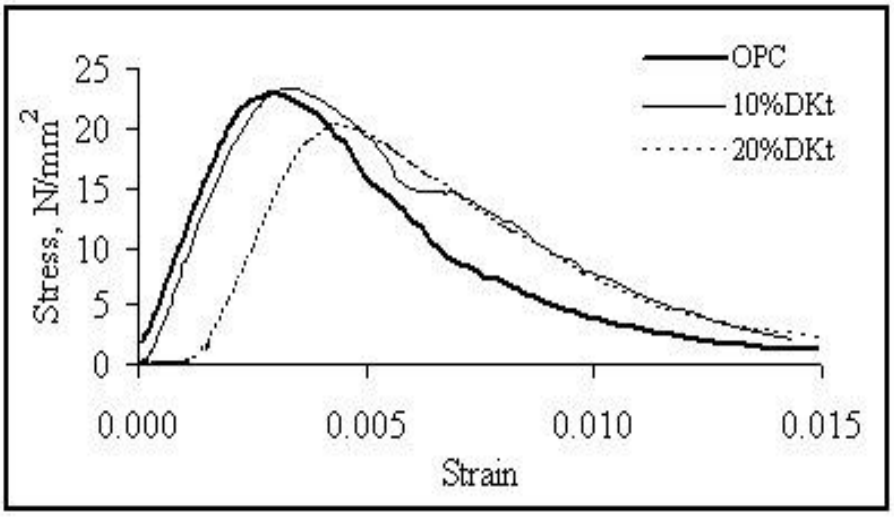

Figure 4.65 Stress-Strain curve of OPC concrete containing different content of DK.

10%DKt inclusion had led to increase the concrete toughness, where the area under the 10%DKt concrete curve was higher than that for OPC concrete. This means that the inclusion of 10%DKt delay the crack propagation. This finding agrees with the above obtained results from the 4-points bending test (vertical displacement, CMOD and CTOD).

On the other hand, Figure 4.65 shows that the stress strain behavior of the concrete containing 20%DKt seems to be different from that containing 10%DKt, where the inclusion of 20%DKt has led to decrease the peak load of OPC concrete. Moreover, the slop of the ascending part shown in the Figure is lower than that of OPC concrete. This means that the stiffness is decreased when OPC was partially replaced by higher amount of DKt (20%). While, the descending part of the stress-strain curve of 20%DKt concrete seems to be similar to that of 10%DKt concrete and less steeper than that of OPC concrete, which means that 20%DKt concrete is less brittle than that of OPC.

4.5.2.5 Modulus of elasticity

The modulus of elasticity of OPC concrete containing different contents of DKt (0, 10 and 20% by mass of OPC) was evaluated according to the Italian Standard UNI EN 12390-6. the test aimed to investigate the effect of DK inclusion on the elastic modulus of OPC concrete at a curing age of 28 days The values of the elastic modulus of the studied concretes are shown in Table 4.7 As should have been expected from the above mentioned results obtained from stress-strain curve of both OPC and 10%DKt concrete, the value of elastic modulus of 10%DKt concrete is quit similar to that of OPC concrete. This means that the stiffness of the OPC concrete does not significantly changed by 10%DKt inclusion. On the other hand, 20%DK inclusion decreases the elastic modulus with higher percentage (49.0%). This means that the stiffness of the OPC concrete was significantly decreased by 20%DKt inclusion.

Table 4.7 Elastic modulus of OPC concrete containing different contents of DKt.

Concrete property	DKt content, %		
	0	10	20
Elastic modulus, GPa	27.596	27.865	14.191

4.5.2.6 Shrinkage

Figure 4.66 shows drying shrinkage strain of DKut and SF concrete made with a constant w/b ratio of 0.5 after water curing period of 28 days The results shown in the figure indicate that the drying shrinkage of the concrete containing 5%DKut was found to be closed to or somewhat lower than that of OPC concrete. Moreover, the amount of reduction in the dry shrinkage was increased when OPC was replaced by higher percent of DKut (10%). The

measured drying shrinkage strain after a period of 336 days was found to be 480, 470 and 455 microstrain for OPC, 5%DKut and 10%DKut concrete, respectively. Figure 4.65 also shows that the rate of drying shrinkage for all studied concrete was decreased rapidly with time, where 60 percent of the final drying shrinkage strain was realized in the first 3 months. The drying shrinkage of SF concrete is comparable to that of the control concrete where, the value of the measured drying shrinkage strain was found to be 475 microstrain (Figure 4.66).

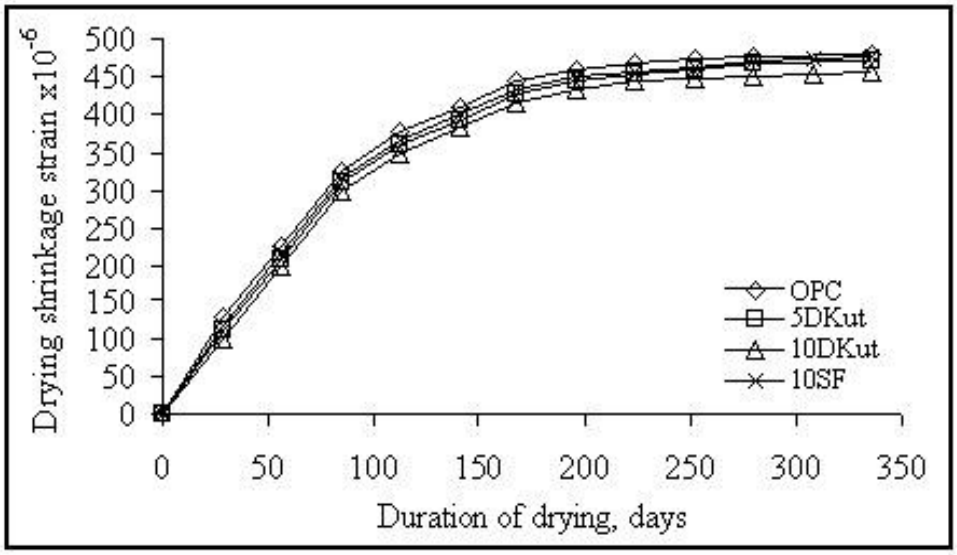

Figure 4.66 Drying shrinkage of OPC concrete containing either DKut or SF.

4.5.3 Fluid Transport Properties

The fluid transport properties of DKut concrete were assessed through measuring its water absorption using the sorptivity and initial surface absorption approaches as discussed below.

4.5.3.1 Sorptivity

Figure 4.67 shows the sorptivity of OPC, OPC/DKut and OPC/SF concrete after 28 and 90 days. The figure illustrates that the sorptivity of the OPC concrete decreases with incorporating either DKut or SF and with increasing curing period. The maximum amount of reduction reaches 11 and 55% for OPC concrete containing 10%DKut and 10%SF, respectively.

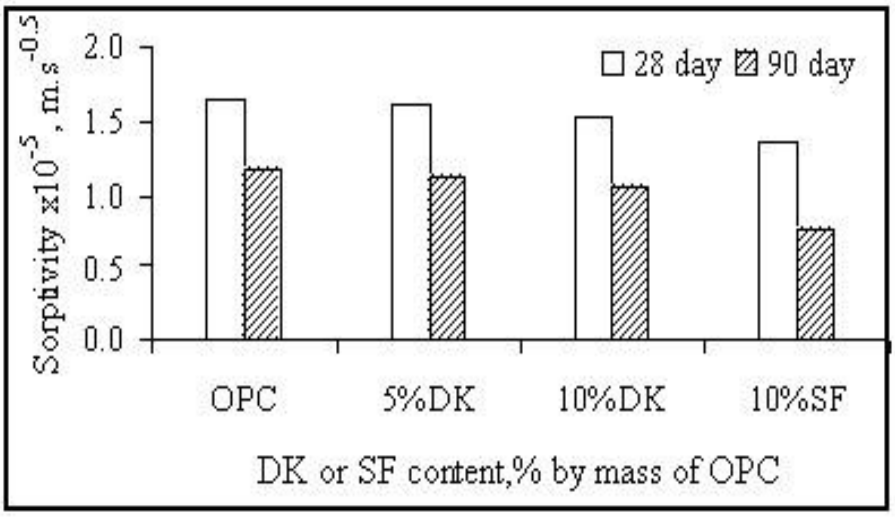

Figure 4.67 Effect of incorporating either DKut or SF on 28 and 90 days sorptivity of OPC concrete

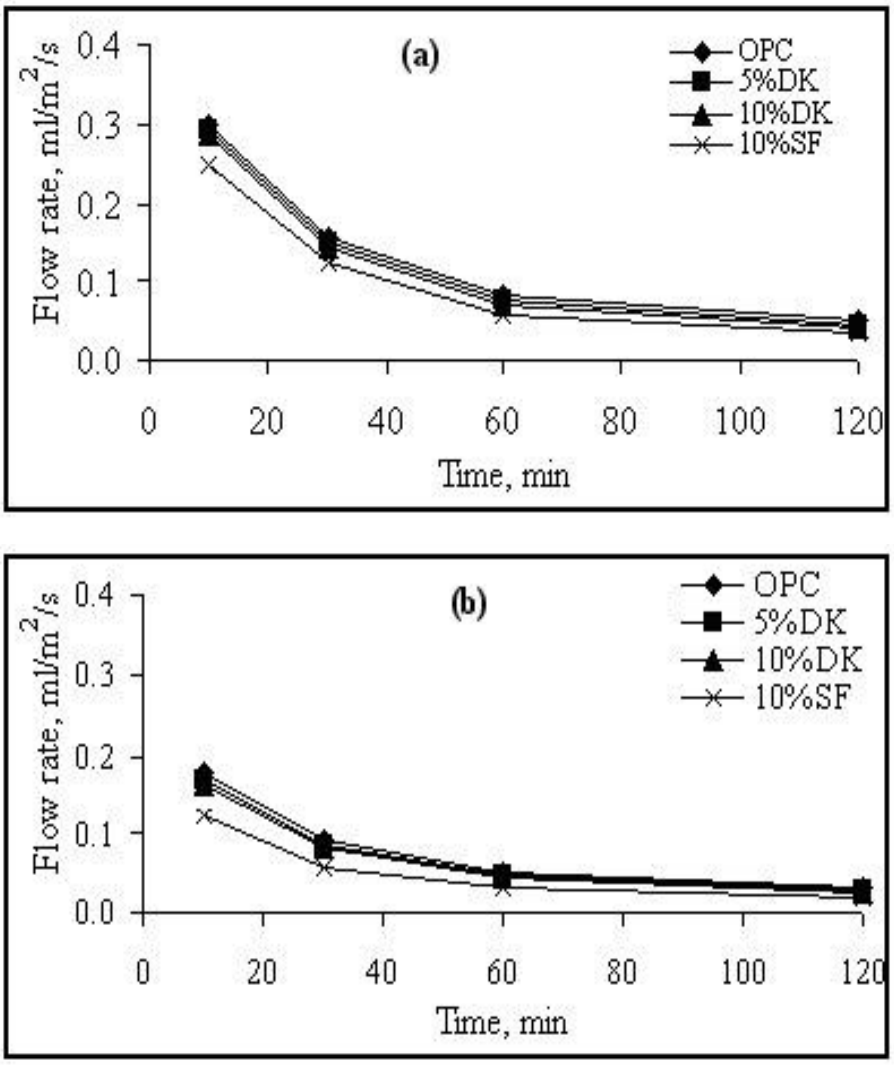

Figure 4.68 Water flow rate at different times from starting testing for OPC, OPC/DK and OPC/SF concrete after a)28 days and b)90 days.

4.5.3.2 Surface water absorption

To confirm the sorptivity results, the mass transport properties for similar sorptivity concrete specimens made from the same studied mixes were also investigated using the initial surface absorption test (ISAT). Figure 4.68 shows the flow rate of water for OPC, OPC/DKut and OPC/SF concrete after 28 and 90 days curing period as a function of time from starting the test. The figure illustrates that the flow rate of water decreases with increasing the time from starting the test, incorporating either DKut or SF and with increasing the curing period. Rate of reduction in the water flow rate decreases with time. The maximum amount of reduction occurs by replacing OPC by 10% SF followed by 10%DKut.

Figure 4.69 illustrates the flow rate of water at 10 minutes ($ISAT_{10}$) for OPC, OPC/DKut, and OPC/SF concrete specimens at the age of 28 and 90 days. It is clear from the results that the inclusion of DKut in OPC concrete had led to a slight reduction in their $ISAT_{10}$ values. The maximum amount of reduction achieved by replacing OPC by 10% SF followed by 10%DKut.

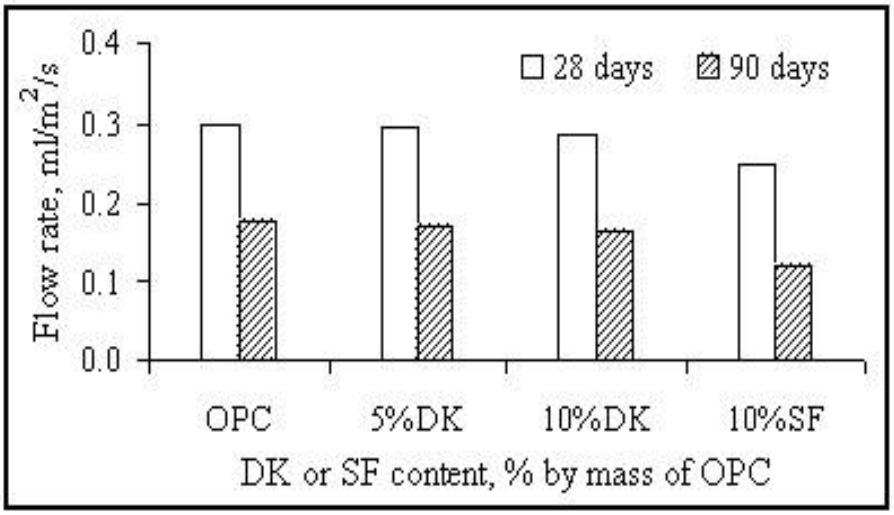

Figure 4.69 Water flow rate (ISAT10) for OPC, OPC/DKut and OPC/SF concrete cured in water for 28 and 90 days.

CHAPTER 5
RESULTS DISCUSSION

5.1 INTRODUCTION

This chapter explains and discusses all obtained results analyzed in chapter 4.

5.2 THE CHARACTERIZATION OF DALUMINATED KAOLIN

Kaolin is a natural clay mineral composed of aluminosilicate with well defined lattice parameters identified by means of X-ray diffraction. The calcination of kaolin at ~700^{o}C leads to its dehydroxylation and leaves behind unstable amorphous structure susceptible to react with basic oxides to form more stable configurations. When properly activated, the calcined kaolin, known as metakaolin, possesses good pozzolanic properties and is a well known artificial pozzolana.

The most important characteristic of the calcined kaolin is the chemical composition (SiO_2 + Al_2O_3 about 90-95%). In the alum industry, aluminum is extracted from the calcined kaolin as soluble aluminum sulfate through treatment with sulfuric acid. The dealumination process is not carried out in the natural mineral because of its stable structure whilst the amorphous state of the calcined solid facilitates the extraction process (Colina and Llorens, 2007). The dealuminated kaolin (DK) waste is a silica-rich solid, acidic in nature and contains some residual aluminum which has not been extracted. As a result of the acid attack, the silica is present in a disordered non-polymerized weakly- or non- bonded form. The surface area of the multiphase waste is high due to the fine particulates left after the acid treatment in addition to the amorphous nature of the heat treated mineral (Colina et al, 2002).

The potential of the waste to bind calcium and hydroxyl ions is high. The binding capacity follows several mechanisms including neutralization and salt formation. During the neutralization process the hydrogen ions adsorbed on the surface of the acidic particulates are replaced by hydroxyl ions, the trivalent aluminum ions transforms to aluminate and the aluminates react with calcium to precipitate calcium aluminate hydrates of weak cementing properties which in the presence of gypsum they form ettringite. The described mechanism differs totally from that of silica fume with lime, where the pure condensed fume of silica react to form calcium silicate hydrate with strong cementing properties (Mostafa et al, 2001a).

Under these conditions, the binding capacity of lime, known generally as the pozzolanic reactivity, cannot be interpreted exclusively as an initiator for the polymerization of the weakly bonded silica to form the calcium silicate hydrates. It involves also the neutralization process as well as the formation of gypsum, calcium aluminate hydrates and ettringite.

Several differences exist between the DK and the silica fumes and lead to different reaction mechanisms among which the presence of alumina in acidic DK is to be mentioned. The nature of the amorphous character in both materials is variable; the microsilica is an agglomeration of condensed fume but the DK is a result of the acid treatment of a calcined kaolin.

5.3 SETTING BEHAVIOR OF OPC/DK PASTE

The setting time of OPC depends on the phase composition, the concentration of the liquid phase and the pH-value; the amount of alkalis, lime, and soluble alumina play dominant role in the process. Setting is accelerated by alkali hydroxides and soluble alumina; it is retarded by lime, ferric hydroxide, and other anions such as sulfates and borates. Excess sulfates lead to secondary gypsum and cause false setting. Setting is delayed by fly ashes possibly due to the presence of carbon particles in the ashes and is prolonged by silica fume (Neville, 1998).

The DK contains a significant content of alumina compared to OPC (13% Al_2O_3 in DKut, 16% in the DKt, 5.59% in the OPC). As previously mentioned, the alumina of the acidic DK (DKut) is in the form of soluble aluminum sulfate which upon replacement of part of OPC it increases the crystalline character of the hydration products and accelerates the hydration and setting. On the other hand, the lime treated DK contains calcium sulfoaluminate hydrates and excess lime which delay setting.

In general, the natural pozzolana accelerates the rate of hydration of the clinker. The surface area of the material, its chemical composition and physical state of the surface, the more or less rapid release of alkalis, contribute to the acceleration of the initial hydration rate of cement. The DK addition leads to an increase in the water demand of the paste due to the higher surface area with a consequent contribution in the acceleration of the rate of hydration. The total heat evolved is attributed to the heat of reaction and the heat of neutralization.

5.4 FRESH PROPERTIES OF OPC/DK SYSTEM

Pozzolanic materials with fineness similar to that of Portland cement do not lead to a significant change in its workability. Very fine substances such as microsilica and diatomaceous earths increase the water demand dramatically and decrease the flowability. The pozzolanic reactivity is indicated by the surface area and potential reactivity with lime. Although the surface area of the DK is almost double that of silica fumes, the workability of the OPC mortar does not vary with the addition of the untreated DK and is negatively affected by that of the lime treated (DKt) and strongly affected by SF. This result is explained by the acidic character of the DKut which encompasses fine precipitated salts and grains of high surface area with no cementing properties.

The difference in the flowability of mixes with DK and SF mixes is attributed to the difference in the structure and the nature of the amorphous silica in these materials (Mostafa et al, 2001a). The amorphous silica in the DKut has a lower degree of polymerization than that in SF. The presence of hydroxylated silica surface in the DKut can hold water as was observed by other researchers in the infrared spectrometer (IR) spectra (Mostafa et al, 2001a). The flowability of OPC decreases in presence of the neutralized DK and approaches the performance of SF.

5.5 MICROSTRUCTURE OF OPC/DK HARDENED PASTE

5.5.1 Hydration products

The results obtained from the thermal analysis indicate that the DK act as a pozzolanic material in the OPC-matrix. It reacts with the CH liberated from the hydration reaction of cement and form CSH. As a consequence an increase in the amount of nonevaporable water (NEW) and calcium silicate hydrate (CSH) with the reduction in the calcium hydroxide (CH) content is observed.

The results agree with those obtained by Mostafa et al (2001a) who studied the affinity of DK towards lime in suspension using isothermal conduction calorimetry and accelerated chemical method. The unreacted lime and combined water (NEW) were determined with time. The XRD diagrams indicated the appearance of traces of gehlenite hydrate (C_2ASH_8) with a weak diffraction line at 31 (2θ) in cement pastes containing either DKut or DKt addition. An increase in the amount of the gehlenite phase was observed with the DKut addition and was attributed to high percentage of SiO_2 and Al_2O_3 in the DK (Sersale and Orsin, 1968).

In the present work the EDAX analysis performed on OPC/DK paste showed a composition of Ca, Si and traces of Al, Fe and S at the aggregate-paste interface as well as for the bulk of the sample. A decrease in the Ca/Si ratio was observed with the DK incorporation in the paste. The magnitude of reduction is higher with increasing DK content. A greater amount of CSH formation is therefore favored through the reaction of DK with the lime released from the OPC. The formation of the ettringite is probable due to the presence of calcium, aluminum and sulfate in the paste.

The SEM micrographs (Figures 4.18, 4.19, 4.21 and 4.22) illustrate a decreased amount of platy portlandite crystals with a higher amount of CSH having a sponge-like morphology as well as a slightly higher amount of needle-like crystals typical of ettringite. SEM images show also a lower porous structure with fewer microcracks than that observed in the corresponding OPC paste (Figures 4.17 and 4.20).

The results obtained from SEM showed an improvement in the microstructure of aggregate paste interfacial transition zone (ITZ) for OPC/DK samples. A less porous structure with lower amount of CH and higher amount of CSH was observed than in the corresponding OPC specimen. The reduction in Ca/Si ratio compared to that of hardened cement paste without DKut is thus due to the smaller particle size of DKut allowed to fill the capillaries pores inside the cementitious gel, and forming a higher CSH due to the higher pozzolanic activity of DKut. The incorporation of the SF in the OPC mix increases the amount of NEW and the CSH phases compared to the effect of DK. The decrease in the CH content is much more obvious than in the case of DK.

5.5.2 Pore Structure

The results obtained from the desorption measurements illustrate that the total porosity increases slightly or remains almost unchanged by the DKut addition. This effect is more pronounced for the capillary porosity than the total porosity. The Mercury Intrusion Porosimetry (MIP) test results (Figure 4.26) confirm these findings and show an increase in the gel porosity of OPC/DK samples. The decrease in the capillary porosity in the presence of DKut is attributed to the hydration products formed from the pozzolanic reactions and their filling of the pathways between pores which process leads to the reduction in the amount of the interconnected pores (capillary pores). The increase in gel porosity for the DKut mixes reflects the ability of this fine material to refine larger pores. In spite of this improvement,

however, the particle size distribution curves of the OPC paste does not vary significantly with the inclusion of the DK. This is attributed to the increase in the amount of poorly crystallized ettringite formed in presence of Al_2O_3, and SO_4. The ettringite formed exerts an internal pressure and leads to expansion causing formation of microcracks in the paste. The harmful effect of the ettringite restricts the improvement of the microstructure of the OPC/DK paste (Mehta and Monteiro, 2006).

5.6 MECHANICAL PROPERTIES OF OPC/DK SYSTEM

The results obtained from measurements carried out on the mortar and concrete indicates the improvement in the mechanical properties of the OPC-mortars in the presence of DK. This is attributed to the improvement of the tensile strength and the bond strength between the aggregate and the cement paste and the respective microstructure of the cement paste and the aggregate-paste interfacial transition zone.

The mechanical properties are, however, negatively affected with the increase of the DK content as well as at longer curing age. This is attributed to the aluminum ions supplied from the DK and the respective ettringite formation. This explains the decrease in the values obtained in the measurements of the fluid transport properties, mechanical and durability aspects.

5.7 DRYING SHRINKAGE OF OPC/DK CONCRETE

The main causes of the drying shrinkage of the cement paste when exposed to ambient humidity is the removal of adsorbed water from the hydrated cement paste (Neville, 1998 and Mehta and Monteiro, 2006). The pozzolanic materials lead to an increase in the volume of the fine pores of the cement hydration products. The drying shrinkage in concrete are directly associated with the water held by small pores in the size range of 3 to 20 nm. The concrete containing pozzolans cause therefore a pore refinement process usually associated with a higher drying shrinkage.

The DKut acts as a pozzolanic material and tends to refine the pores in the hydrated cement paste. A drying shrinkage of the concrete is therefore expected. The DKut inclusion, however, caused unexpectedly lower drying shrinkage in concrete and the effect is more pronounced with higher DKut content. This is attributed to the formation gypsum formed from the chemical reaction between portlandite and the sulfate ions in DKut (Figure 4.11, 4.12). The

gypsum formation causes expansion in the cement paste and compensates the drying shrinkage. The extent of compensation depends on the amount of gypsum and the amount of DKut in concrete. The positive effect of SF on the drying shrinkage of concrete is attributed to the formation of a denser microstructure of the CSH in the hydrated cement paste, less voids and a consequent less water adsorption. (Grutzeck et al, 1982).

5.8 FLUID TRANSPORT PROPERTIES OF OPC/DK SYSTEM

The replacement of cement by the DK or SF as pozzolanic materials causes a reduction in the fluid transport properties exemplified in the sorptivity (Figures 4.35 and 4.67), water absorption (Figure 4.37) and rate of water flow rate (Figure 4.68). The amount of reduction depends on the type of the material used i.e. on its chemical composition, surface area, pozzolanic reactivity and the mechanism of hydration. The rate of reduction depends also on the replacement ratio.

The reduction in the fluid transport properties of the OPC in the presence of DK is interpreted by the results obtained from thermo-gravimetric, XRD and SEM analysis. The amount of CSH phases increased with decreasing the portlandite content. The larger pores were refined and were converted into discontinuous pores. The capillary porosity of OPC/DK decreased relative to that of OPC.

5.9 DURABILITY OF OPC/DK REINFORCED MORTAR

5.9.1 Sulfate Attack

The compressive strength of the cement mortars and concrete also in the presence of pozzolanic materials increased. Negligible change in the expansion and the weight gained of specimens immersed in water were observed. The compressive strength of the specimens immersed in sodium sulfate solutions showed an initial increase then were reduced at longer exposure ages (see Figure 4.41). This behavior depends on the type of binder used and the replacement ratio of the pozzolanic material. The observed effect is explained by the formation of fine ettringite crystals which fill the pores at first (Neville, 1998 and Mehta and Monteiro, 2006), but increase their volume at longer exposure periods. The internal pressure created lead to expansion, cracking and a consequent reduction in the compressive strength (Mangat and Khatib, 1995). The improvement of the permeation characteristics of HCP in the presence of DK or SF hinder the amount of aggressive ions transported within the matrix and reduce the extent of formation of gypsum and ettringite. The increased expansion of the

OPC/DK systems observed at longer age is attributed to the formation of higher amount of ettringite resulting from the reaction between sulfate ions, aluminate and portlandite. The expansion and weight gain depends on the exposure period to the aggressive ions; the respective values are reduced in specimens subjected to wet/dry exposure compared to those continuously immersed in the aggressive solutions.

5.9.2 Reinforcement Corrosion

The initial reduction observed in the corrosion potential and the corrosion rate of the OPC/DKut specimens is attributed to the depression in the mass transport properties of the mortars as a result of the improvement in the microstructure, pore structure and capillary porosity. The subsequent increase in the corrosion activities is discussed below:

Part of the chloride ions penetrating the concrete cover are bound with the hydration products of cement and others remain free. The free chloride penetrates further into deeper layer by the capillary suction (Schiebl, 1983). The process continues until the ions reach the surface of reinforcing steel and react at anodic sites forming hydrochloric acid which destroys the passive protective film producing localized pits. Once the acidic environment form around the pit, the pit remains active and increases in depth with increasing exposure period (Okba et al, 1993, Abdelaziz, 1993 and Arya and Xu, 1995).

On the other hand the reduction in the calcium hydroxide content of the OPC-DKut paste as a result of the pozzolanic reaction, and with the help of penetrated chloride ions, cause an increase in threshold value (CL^-/OH^-) = 0.30 and a consequent disruption of the passive oxide film on the surface of reinforcement. In the presence of oxygen and moisture the corrosion process takes place (Hussain et al, 1995).

The sulfate ions released from the OPC/DKut hydration products, gypsum and ettringite, have a detrimental role in destroying the passive film by changing it into a weak film (Holden et al, 1983). The presence of these ions in environments containing chloride ions leads to an increase in the rate of corrosion activity of the reinforced concrete and consequently in its degree of degradation.

5.10 IMPROVING PROPERTIES OF OPC/DK SYSTEM

SF was added to DKut in the reinforced OPC mortars to reduce the negative effect of DK. The result showed a beneficial effect; the mechanical properties improved and the degradation of reinforced DK mortar was reduced. This is attributed to the reduction of the gypsum and ettringite formation as a result of depressing the available Al_2O_3. The microstructure therefore improves with a consequent reduction in the porosity and the fluid transport properties of the mix.